Degradable Bioadhesives Based on Star PEG–PLA Hydrogels for Soft Tissue Applications

Mathilde Grosjean, Edouard Girard, Edouard Girard, Audrey Bethry, Grégory Chagnon, Xavier Garric, Benjamin Nottelet

Degradable Bioadhesives Based on Star PEG−PLA Hydrogels for Soft Tissue Applications

Mathilde Grosjean, Edouard Girard, Audrey Bethry, Grégory Chagnon, Xavier Garric, and Benjamin Nottelet*

ABSTRACT: Tissue adhesives are interesting materials for wound treatment as they present numerous advantages compared to traditional methods of wound closure such as suturing and stapling. Nowadays, fibrin and cyanoacrylate glues are the most widespread commercial biomedical adhesives, but these systems display some drawbacks. In this study, degradable bioadhesives based on PEG– PLA star-shaped hydrogels are designed. Acrylate, methacrylate, and catechol functional copolymers are synthesized and used to design various bioadhesive hydrogels. Various types of mechanisms responsible for adhesion are investigated (physical entanglement and interlocking, physical interactions, chemical bonds), and the adhesive properties of the different systems are first studied on a gelatin model and compared to fibrin and cyanoacrylate references. Hydrogels based on acrylate and methacrylate reached adhesion strength close to cyanoacrylate (332 kPa) with values of 343 and 293 kPa, respectively, whereas catechol systems displayed higher values (11 and 19 kPa) compared to fibrin glue (7 kPa). Bioadhesives were then tested on mouse skin and human cadaveric colonic tissue. The results on mouse skin confirmed the potential of acrylate and methacrylate gels with adhesion strength close to commercial glues (15–30 kPa), whereas none of the systems led to high levels of adhesion on the colon. These data confirm that we designed a family of degradable bioadhesives with adhesion strength in the range of commercial glues. The low level of cytotoxicity of these materials is also demonstrated and confirm the potential of these hydrogels to be used as surgical adhesives.

1. INTRODUCTION

The treatment of tissue wounds constitutes an important clinical challenge. Tissue wounds range from minor skin cuts to severe injuries and can result from various causes, such as traumatic incidents, surgical incisions, or chronic wounds like diabetic ulcers, for example.[1] These injuries are usually treated through the reconnection of the injured tissues and closure of the defect area. The main objectives are to stop bleeding, prevent leakage, and also restore tissue structure and function.[2]

Tissue adhesives are interesting materials for wound treatment as these systems present various advantages compared to traditional methods of wound closure, such as suturing and stapling.[3] Indeed, they allow the tissue damage to be minimalized and can be applied easier and faster. Moreover, bioadhesives can also act as a hemostatic agent or physical barrier to prevent leakage. However, their use stays restricted because of several limitations,[4] such as weak adhesion or poor mechanical properties.

Tissue adhesives can be based on either natural or synthetic polymers. Natural bioadhesives include fibrin, collagen, gelatin, albumin, and chitosan systems, whereas synthetic ones mainly comprise polyurethane, polyethylene glycol, and cyanoacrylate.[5,6] Both covalent and noncovalent interactions can be responsible for tissue adhesion properties. In the first case, various reactive groups can be used to react with tissue functional groups and achieve covalent cross-linking. For example, cyanoacrylates possess an unsaturated carbon double bond that can react with amine groups of tissues through a Michael addition.[7] Other systems are based on *N*-hydroxysuccinimide (NHS) esters that can undergo a spontaneous reaction with primary amines of living tissues to form amide bonds.[3] Aldehyde groups can also react with amines to form imine bonds.[8] Finally, adhesive systems can contain catechol moieties that can be oxidized to quinones, which are able to react with amines, thiols, and imidazoles of tissues through various pathways (Michael addition and Schiff base reaction).[9] Regarding noncovalent interactions, physical polymer entan-

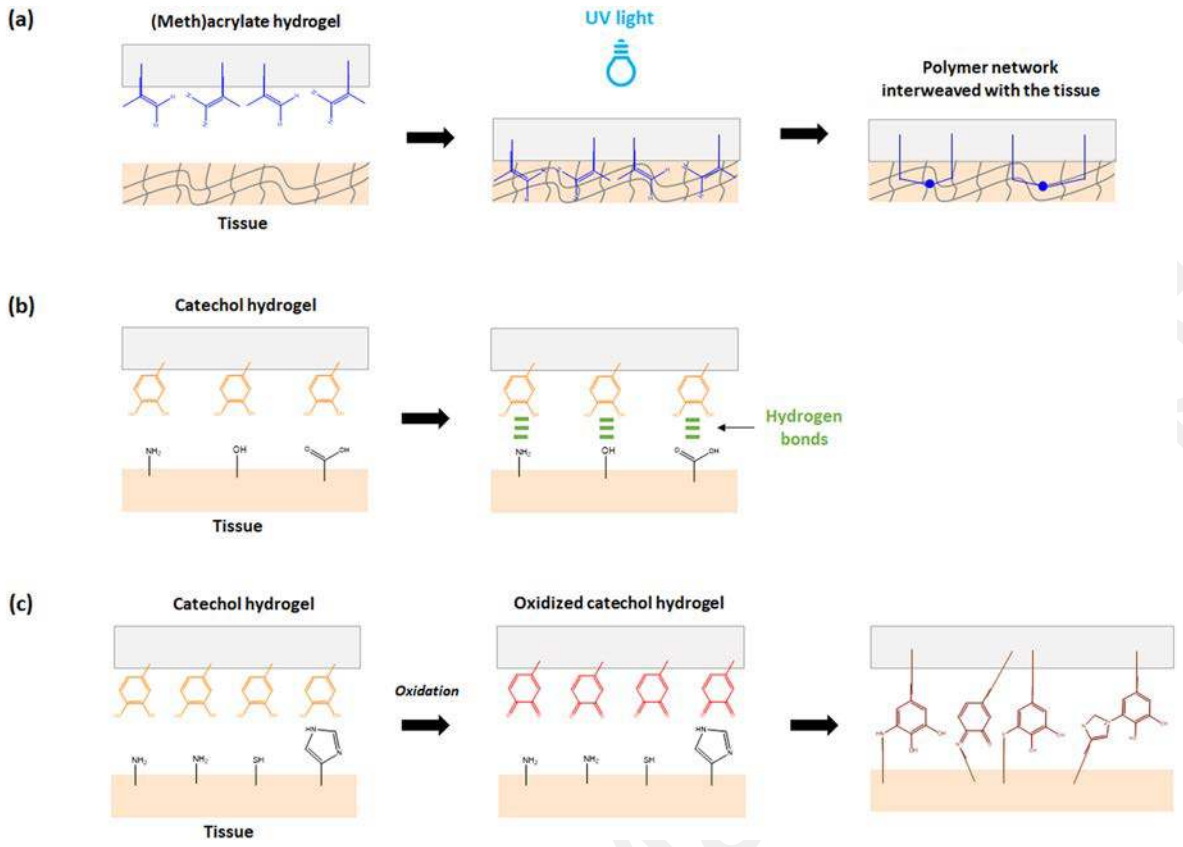

Figure 1. Different mechanisms responsible for tissue adhesion based on the functional groups used in this work: (a) physical entanglement and interlocking (meth(acrylate)-based hydrogels); (b) hydrogen bonds (catechol-based hydrogels); (c) covalent linkages (oxidized catechol-based hydrogels).

glement, and mechanical interlocking, hydrogen bonding and hydrophobic interactions can be responsible for adhesion properties. One major example of bioadhesives based on the mechanism of physical entanglement are acrylate-based systems.[10] Polymers containing acrylates first diffuse into the tissue and are then cross-linked to create a polymer network interpenetrated with the tissue. Common examples of adhesive systems that can form hydrogen bonds with tissues are based on acrylic acid because of the presence of carboxylic acid groups.[11,12]

Nowadays, fibrin and cyanoacrylate glues are the most popular bioadhesives. However, both of these systems show limitations. Fibrin glues are expensive and suffer from limited adhesion strength and compatibility issues since they are based on fibrinogen, which is most of the time derived from human plasma. Other systems are derived from bovine substances but present a risk of allergic reaction.[3] Cyanoacrylates are well-known for their high adhesion but their lack of degradability and toxicity limits their use to skin applications. To overcome these issues, poly(ethylene glycol) and polyester derivatives appeared as interesting substitutes.[6,13−20] However, it remains difficult to find a compromise between appropriate hydrophilicity, adhesiveness, and suitable mechanical properties.[3] In the category of PEG derivatives, a first example reported the use of PLA−PEG−PLA or PGA−PEG−PGA triblock copolymers terminated with acrylate groups.[13] However, these adhesives were very soft or viscous liquids. The first commercial tissue adhesive based on PEG was then designed. The product, called FocalSeal, was approved by the FDA in 2000.[6] The system is composed of PEG−PLA and PEG−PTMC prepolymers and required the use of eosin Y as photoinitiator. FocalSeal was discontinued due to the low compliance of surgeons as the application process involved multiple steps but also for biocompatibility issues linked to the free radical polymerization process.[21] Other bioadhesives based on PEG often use amine/NHS ester[6] or thiol/NHS ester systems[14] to achieve covalent cross-linking. For example, the commercial product DuraSeal based on 4-armed star-PEG functionalized with NHS esters and trilysine was developed and approved by the FDA in 2005.[22] Because NHS esters require dry storage to be protected from hydrolysis, the application involved a multiple step preparation and long application time. Moreover, the important swelling of PEG-based adhesives appeared to be an important drawback. Regarding polyesters, they are often modified with acrylates[15,18,23] or isocyanates.[19] While acrylates are able to quickly cross-link upon UV irradiation, isocyanates display high reactivity with amines from living tissues. Other examples of polyester adhesives reported the use of NHS ester.[16,20] These systems showed greater adhesion strength compared to fibrin glue but lower than cyanoacrylate. Other research also focused on the development of polyether and/or polyester systems functionalized with catechol moieties. For instance, biodegradable adhesive polymers composed of 3,4-dihydroxyphenylalanine derivatives, PEG, and PCL were reported.[24] In this case, the arms of a 4-armed PEG were grafted with either catechol groups or PCL chains yielding macromolecular structures with nonhomogenous composition and functionality but showing adhesive properties.

In this work, our objective is to take advantage of multifunctional amphiphilic PEG−PLA copolymers to design new biodegradable and bioadhesive formulations and overcome the issues encountered by current fibrin, cyanoacrylate, PEG, or PEG−polyester glues. We selected PEG thanks to its recognized biocompatibility and its swelling abilities that can participate in the adhesion mechanism through local dehydration of the tissues.[25] PLA was chosen in view of its degradability and hydrophobicity leading to hydrophobic domains in the gels that act as network nodes and improve the gels mechanical properties even for low degrees of polymerizations.[26,27] We also want to design multifunctional copolymers with a high number of well accessible groups responsible for adhesion. To this aim, a degradable 8-arm star-shaped PEG−*b*-PLA copolymer of selected EG/LA composition is prepared and functionalized with various reactive moieties. The star morphology was selected as star-shaped copolymers are known to display higher mechanical properties compared to their linear counterparts.[28−30] Moreover, the high number of chain-ends allow a multifunctionalization of the copolymers, which increases the possibilities of interaction with the tissues. First, acrylic and methacrylic groups are used to yield photocurable bioadhesive gels, where the adhesive properties are based on physical entanglement and interlocking (Figure 1a). In this case, the polymer can first diffuse into the tissue before creating an interpenetrated network after cross-linking. Alternatively, catechol functions have been chosen as they are well-known for their bioadhesion properties.[31−33] The first system is only based on hydrogen bonds that can occur between catechol groups and the different surface chemical groups of living tissues (Figure 1b). In a second system, catechol moieties are oxidized to quinones to obtain an adhesive able to create covalent linkages through Michael addition and Schiff base reaction with the tissues (Figure 1c). Compared to (meth)acrylate derivatives, the advantage of catechol bioadhesives is the absence of UV irradiation, which could lead to cell toxicity depending on the site of application. The copolymers are fully characterized before being used to design bioadhesive hydrogel formulations. The designed systems are not yet intended for a defined application, and the main objective of the study is to assess the adhesive properties of the gels and compare them with commercial glues with very different adhesion properties to explore their potential. Therefore, the adhesion strength of the various gels is next assessed on gelatin, mouse skin, and human cadaveric colonic tissue. The cytotoxicity and degradability are finally evaluated to further confirm the applicability of these hydrogels as degradable bioadhesives for soft tissue applications. Depending on the results obtained, the final application could be targeted more precisely and further investigations could be set up in the future to pursue the development of the adhesive hydrogel system.

2. MATERIALS AND METHODS

2.1. Materials. D,L-Lactide was purchased from Corbion (Gorinchem, The Netherlands). Hydroxyl-terminated eight-armed poly(ethylene glycol) (tripentaerythritol) (PEG_{8arm}20k, M_w = 20 000 g·mol^{-1}) was purchased from JenKem Technology Co., Ltd. (Beijing, China). Tin(II) 2-ethylhexanoate ($Sn(Oct)_2$), triethylamine (Et_3N), methacryloyl chloride, acryloyl chloride, dopamine hydrochloride, *N*-acetyl-DL-homocysteine thiolactone (citiolone), Celite 545, toluene, dichloromethane (DCM), diethyl ether (Et_2O), tetrahydrofuran (THF), and *N*,*N*-dimethylformamide (DMF) were purchased from Sigma-Aldrich (St Quentin Fallavier, France). All chemicals were used without further purification with the exception of toluene and DCM which were dried over calcium hydride and freshly distillated before use. Tisseel (Baxter) fibrin glue and Leukosan Adhesive cyanoacrylate glue were provided by MD Edouard Girard and used as a control for the evaluation of adhesive properties.

2.2. Characterization. Average molecular weights ($\overline{Mn}$) and dispersities ($Đ$) were determined by size exclusion chromatography (SEC, Shimadzu SIL-20A HT) using two mixed medium columns PLgel 5 μm MIXED-C (300 × 7.8 mm), a Shimadzu RI detector 20-A, and a Shimadzu UV detector SPD-20A (260 and 290 nm) (40 °C thermostatic analysis cells). THF was the mobile phase with 1 mL·min^{-1} flow at 30 °C (column temperature). Polymer was dissolved in THF to reach 5 mg·mL^{-1} concentration; afterward, the solution was filtered through a 0.45 μm Millipore filter before injection. $\overline{Mn}$ and $Đ$ were expressed according to calibration using polystyrene standards.

^{1}H nuclear magnetic resonance (NMR) spectra were recorded at the Laboratoire de Mesures Physiques (LMP) of the University of Montpellier (UM) using a Bruker Avance III HD 400 MHz spectrometer (Bruker, Fällanden, Switzerland) and were calibrated to TMS on the basis of the relative chemical shift of the solvent used as an internal standard. ^{1}H 2D diffusion-ordered (DOSY) NMR spectra were recorded on a Bruker Avance III 600 (Bruker, Fällanden, Switzerland) spectrometer equipped with a 5 mm TCI Prodigy Z-gradient cryoprobe. The standard gradient amplifier (GREAT 1/10-E) generates a maximum gradient strength of 65.7 G cm^{-1} at a current of 10 A. The gradient strengths were calibrated using a sample of D2O 99.96% deuterated from Eurisotop (Saint-Aubin, France). Diffusion measurement was performed with double stimulated echo and bipolar gradient pulses for convection compensation and Eddy current delay (dstebpgp) in a pseudo 2D mode and processed with the Bruker software T1/T2 package from Topspin3.6.2 (Bruker). For this experiment, 16 dummy scans and 32 scans were used with a relaxation delay of 3 s. Diffusion time Δ was fixed to 0.3 s and gradient strength δ, to 2.8 ms. Sinusoidal shapes were used for the gradients, and a linear gradient ramp with 16 increments between 2% and 95% was applied for the diffusion relevant gradients. The diffusion coefficients were calculated with the Bruker software package T1/T2 from Topspin 3.6.2 (Bruker). All diffusion coefficients were within an error range of ±5%.

Thermal properties of the polymers were analyzed by different scanning calorimetry (DSC) using a Mettler Toledo DSC 3 STAR System instrument. Analyses were carried out under nitrogen atmosphere. Samples were heated from 0 to 100 °C (10 °C·min^{-1}) and then cooled to −80 °C (10 °C·min^{-1}) before a second heating ramp to 200 °C (5 °C·min^{-1}). The glass transition temperature (T_g) or melting temperature (T_m) was measured on the second heating ramp.

Viscosity measurements were performed using a Thermo Fisher HAAKE MARS rheometer with a cone−plate geometry with a diameter of 35 mm and 2° cone angle. The values of viscosity were measured at 25 °C at a shear rate of 10 s^{-1}.

The UV-absorbance spectra were obtained using a PerkinElmer Lambda 35 UV/vis spectrometer (200−600 nm).

2.3. Synthesis of the Copolymers. For sake of clarity, PLA_x corresponds to PD,L−LA (also known as PLA50, i.e., 50% of L and D units) with a degree of polymerization DPn = *x*.

2.3.1. PEG_{8arm}20k−$(PLA_{13})_8$ (PEG_{s8}−PLA). Star-shaped copolymer PEG_{8arm}20k−$(PLA_{13})_8$ (PEG_{s8}−PLA) was synthesized by ring opening polymerization (ROP) in solution as described in a recent article from our group.[34]

2.3.2. Methacrylate Functional PEG_{8arm}20k−$(PLA_{13})_8$−MC (PEG_{s8}−PLA−MC). The methacrylate functional PEG_{8arm}20k−$(PLA_{13})_8$−MC (PEG_{s8}−PLA−MC) was synthesized according to a procedure already reported by our group.[34]

2.3.3. Acrylate Functional PEG_{8arm}20k−$(PLA_{13})_8$−AC (PEG_{s8}−PLA−AC). The 8-arm star block copolymer PEG_{s8}−PLA was solubilized in toluene (10% w/v). Determined amounts of Et_3N (15 eq./OH group) were added. The mixture was then cooled at 0 °C before adding acryloyl chloride with a dropping funnel (15 eq./OH group). After 2 h, the mixture was heated to 35 °C for 72 h under

stirring in the dark. Then, the reaction medium was filtered on Celite 545 before being washed with distilled water and concentrated. Afterward, the mixture was precipitated in cold Et_2O. The acrylate functional $PEG_{8arm}20k-(PLA_{13})_8-AC$ ($PEG_{s8}-PLA-AC$) was recovered by filtration and dried under reduced pressure to constant mass.

The functionalization was confirmed by ^1H NMR and DOSY-NMR.

The yield of functionalization was determined by comparing the integration of the signals characteristic of the acrylate at 6.4, 6.1, and 5.8 ppm and the integration of proton resonance at 3.6 ppm of the ethylene glycol unit.

^1H NMR (400 MHz; $CDCl_3$): δ (ppm) = 6.4 (d, 1H, CO−CH═C$\underline{\boldsymbol{H}}_2$), 6.1 (m, 1H, CO−C$\underline{\boldsymbol{H}}$═$CH_2$), 5.8 (d, 1H, CO−CH═C$\underline{\boldsymbol{H}}_2$), 5.1 (q, 1H, CO−C$\underline{\boldsymbol{H}}$−$(CH_3)$−O), 4.3 (m, 2H, O−$CH_2$−C−C$\underline{\boldsymbol{H}}_2$−O), 4.3 (m, 1H, C$\underline{\boldsymbol{H}}$−OH), 3.6 (s, 4H, C$\underline{\boldsymbol{H}}_2$−C$\underline{\boldsymbol{H}}_2$−O), 3.3 (m, 2H, O−C$\underline{\boldsymbol{H}}_2$−C−$CH_2$−O), 1.5 (t, 3H, CO−CH−(C$\underline{\boldsymbol{H}}_3$)−O).

2.3.4. Catechol Functional $PEG_{8arm}20k-(PLA_{13})_8-CT$ ($PEG_{s8}-PLA-CT$). Determined amounts of dopamine hydrochloride (4 eq./acrylate group) and citiolone (4 eq./acrylate group) were solubilized in DMF before Et_3N was added (8 eq./acrylate group). The mixture was stirred overnight at room temperature. Then, $PEG_{s8}-PLA-AC$ was added (10% w/v) and allowed to react at room temperature for 24 h under stirring in the dark. After the total evaporation of DMF, the polymer was solubilized in DCM before being washed with distilled water and concentrated. Afterward, the mixture was precipitated in cold Et_2O. The catechol functional $PEG_{8arm}10k-(PLA_{13})_8-CT$ ($PEG_{s8}-PLA-CT$) was dried under reduced pressure to constant mass.

The functionalization was confirmed by ^1H NMR and DOSY-NMR.

The yield of functionalization was determined by comparing the integration of signals characteristic of the catechol at 6.6 and 6.4 ppm and the integration of proton resonance at 3.6 ppm of the ethylene glycol unit.

^1H NMR (400 MHz, DMSO-d_6): δ (ppm) = 8.8 (d, 1H, CH−N$\underline{\boldsymbol{H}}$−CO−$CH_3$), 8.1 (m, 1H, CO−N$\underline{\boldsymbol{H}}$−$CH_2$−$CH_2$), 6.6 (m, 2H aromatic ring, C$\underline{\boldsymbol{H}}$−C−OH), 6.4 (m, 1H aromatic ring, C−C$\underline{\boldsymbol{H}}$═CH−C−OH), 5.2 (q, 1H, CO−C$\underline{\boldsymbol{H}}$−$(CH_3)$−O), 4.3 (m, 2H, O−$CH_2$−C−C$\underline{\boldsymbol{H}}_2$−O), 4.4 (t, 1H, C$\underline{\boldsymbol{H}}$−NH−CO−$CH_3$), 3.5 (s, 4H, C$\underline{\boldsymbol{H}}_2$−C$\underline{\boldsymbol{H}}_2$−O), 3.3 (m, 2H, O−C$\underline{\boldsymbol{H}}_2$−C−$CH_2$−O), 3.2 (m, 2H, CO−NH−C$\underline{\boldsymbol{H}}_2$−CH), 2.7 (m, 2H, CO−C$\underline{\boldsymbol{H}}_2$−$CH_2$−S), 2.7 (m, 2H, CO−$CH_2$−C$\underline{\boldsymbol{H}}_2$−S), 2.7 (m, 2H, S−C$\underline{\boldsymbol{H}}_2$−$CH_2$−CH), 2.7 (m, 2H, NH−$CH_2$−C$\underline{\boldsymbol{H}}_2$−C), 2.1 (m, 2H, S−$CH_2$−C$\underline{\boldsymbol{H}}_2$−CH), 1.8 (s, 3H, CH−NH−CO−C$\underline{\boldsymbol{H}}_3$), 1.5 (t, 3H, CO−CH−(C$\underline{\boldsymbol{H}}_3$)−O).

2.4. Preparation of the Gels. *2.4.1. Catechol-Based Hydrogels.* Catechol physical gels (CT-Gel) were simply obtained my mixing $PEG_{s8}-PLA-CT$ with water at different concentrations (10, 15, and 20 wt %).

Oxidized catechol gels (CT_{OX}-Gel) were prepared by mixing $PEG_{s8}-PLA-CT$ with $NaIO_4$ solution ($n_{catechol} = n_{NaIO4}$) at different concentrations (10, 15, and 20 wt %). The oxidation of catechol moieties was confirmed by UV−vis spectroscopy.

2.4.2. Acrylate- and Methacrylate-Based Photocurable Gels. Acrylate and methacrylate photocurable gels (AC-Gel and MC-Gel, respectively) were prepared by mixing $PEG_{s8}-PLA-MC$ or $PEG_{s8}-PLA-AC$ with water at different concentrations (5, 10, 15, and 20 wt %). Then, the solutions were irradiated under UV light for 10 min with a Dymax QX4 system (LEDs irradiating at 365, 385, and 405 nm) to obtain 5 mm thick photo-cross-linked gels. The distance measured between LEDs and samples was 3 cm.

The resulting gels were dried before being weighed and put in DCM (5 mL). After 24 h, the insoluble cross-linked parts were removed from DCM and dried under vacuum. Finally, samples were weighed to determine the gel fraction according to eq 1.

$$\text{gel fraction (\%)} = \frac{\text{weight of insoluble crosslinked parts}}{\text{weight of initial sample}} \times 100 \quad (1)$$

As a control for the evaluation of the adhesive properties, gels based on the nonfunctional $PEG_{s8}-PLA$ copolymer were also prepared (nF-Gel). In addition, commercial Tisseel (Baxter) fibrin glue and Leukosan Adhesive cyanoacrylate glue were also tested.

2.5. Testing of Adhesive Properties. *2.5.1. Adhesive Testing on Gelatin Coating.* Gelatin coating solution was prepared by dissolving porcine gelatin 20% (w/v) in PBS at 80 °C. The top region (25 × 25 mm^2) of two glass slides was coated with gelatin, which was allowed to dry at room temperature overnight.[35,36] The thickness of the gelatin coating between 70 and 80 μm was verified by a measurement with a micrometer. Afterward, 100 μL of the desired adhesive preparation was applied on the gelatin-coated part of a glass slide before being covered by another gelatin-coated glass slide (Figure 6a), and the formed excess was removed. The photocurable samples were then irradiated under UV light for 5 min with a Dymax QX4 system (LEDs irradiating at 365, 385, and 405 nm). The distance measured between LEDs and samples was 3 cm.

After 10 min, the adhesive properties were tested using the lap shear test on an Instron 3344 testing machine equipped with a 500 N load cell at a rate of 15 mm·min^{-1}. The maximal force of detachment between substrates was recorded, and the corresponding adhesive strength was calculated by normalizing with respect to the area. All tests were replicated at least 3 times.

2.5.2. Adhesive Testing on Mouse Skin. Adhesive testing was performed on fresh mouse skin collected from 3 male BL/6 mice. All animal investigations were approved by the ethics committee of the French Ministry of Education and Research (contract number 02367.01, task order 1065, ecart number 76) and carried out in accordance with European Union Directive 2010/63/EU for animal experiments. The skin was cut into rectangular specimens (30 × 10 mm) with a scalpel. The area at one extremity of the samples was shaved with a razor.

The adhesion of CT-Gel and CT_{OX}-Gel as well as the references was evaluated with lap-shear test, whereas a tensile test was used for AC-Gel and MC-Gel, which needed to be exposed to UV light. To this end, CT-Gel and CT_{OX}-Gel were applied (25 μL) on the shaved area of a rectangular specimen on a surface of 5 × 5 mm^2 before being covered by a second specimen (Figure 5b), and the formed excess was removed. The same protocol was used for cyanoacrylate and fibrin references. AC-Gel and MC-Gel were applied between the sections (10 × 1 mm^2) of two specimens (Figure 5c) before being exposed to UV light for 5 min with a Dymax QX4 system (LEDs irradiating at 365, 385, and 405 nm). The distance measured between LEDs and samples was 3 cm.

After 10 min, the adhesive properties were tested using the lap shear test on an Instron 3344 testing machine equipped with a 500 N load cell at a rate of 15 mm·min^{-1}. The maximal force of detachment between substrates was recorded, and the corresponding adhesive strength was calculated by normalizing with respect to the area. All tests were replicated at least 3 times.

2.5.3. Adhesive Testing on Cadaveric Colonic Tissue. Cadavers were selected for anatomical dissection from the Anatomy laboratory, Faculty of Medicine, Grenoble, France (LADAF − Laboratoire d'Anatomie des Alpes Françaises). This study was performed in compliance with French regulations of post-mortem testing, and the protocol was approved by a local scientific committee of the Grenoble-Alpes University.

Cadavers were embalmed with a formalin solution (ARTHYL) injected into the carotid artery and drained from the jugular vein (9 L with a formaldehyde concentration of 1.3%) and then preserved in a refrigerated room at 4 °C. Our study includes 2 anatomical dissections, realized on patients aged 89 years, without apparent colonic pathology. The main peritoneal cavity was approached by a median laparotomy. Subtotal colectomy was realized, and specimens were preserved in 0.9% NaCl solution at 4 °C for 13 days. Rectangular specimens (50 × 10 mm) were prepared for analysis.

As described previously, the adhesion of CT-Gel and references was evaluated with the lap-shear test, whereas a tensile test was used for AC-Gel and MC-Gel. CT-Gel, fibrin, and cyanoacrylate glues (50 μL) were applied on the mucous side (inner part) on a rectangular

Table 1. Molecular Weight, Dispersity, and Thermal Properties of the Star-Shaped Copolymers

sample	copolymer	$\overline{Mn}_{NMR}$(g·mol^{-1})	$Đ$	T_g (°C)	T_m (°C)	ΔH_m(J·g^{-1})
PEG_{s8}−PLA	PEG_{8arm}20k−$(PLA_{13})_8$	27 500	1.1	nd[a]	40.5	−60.0
PEG_{s8}−PLA−MC	PEG_{8arm}20k−$(PLA_{13})_8$−MC	27 500	1.1	nd	33.0	−48.2
PEG_{s8}−PLA−AC	PEG_{8arm}20k−$(PLA_{13})_8$−AC	27 700	1.1	nd	41.2	−41.6
PEG_{s8}−PLA−CT	PEG_{8arm}20k−$(PLA_{13})_8$−CT	27 900	1.1	nd	38.4	−40.5

[a]Not detected under the conditions of analysis.

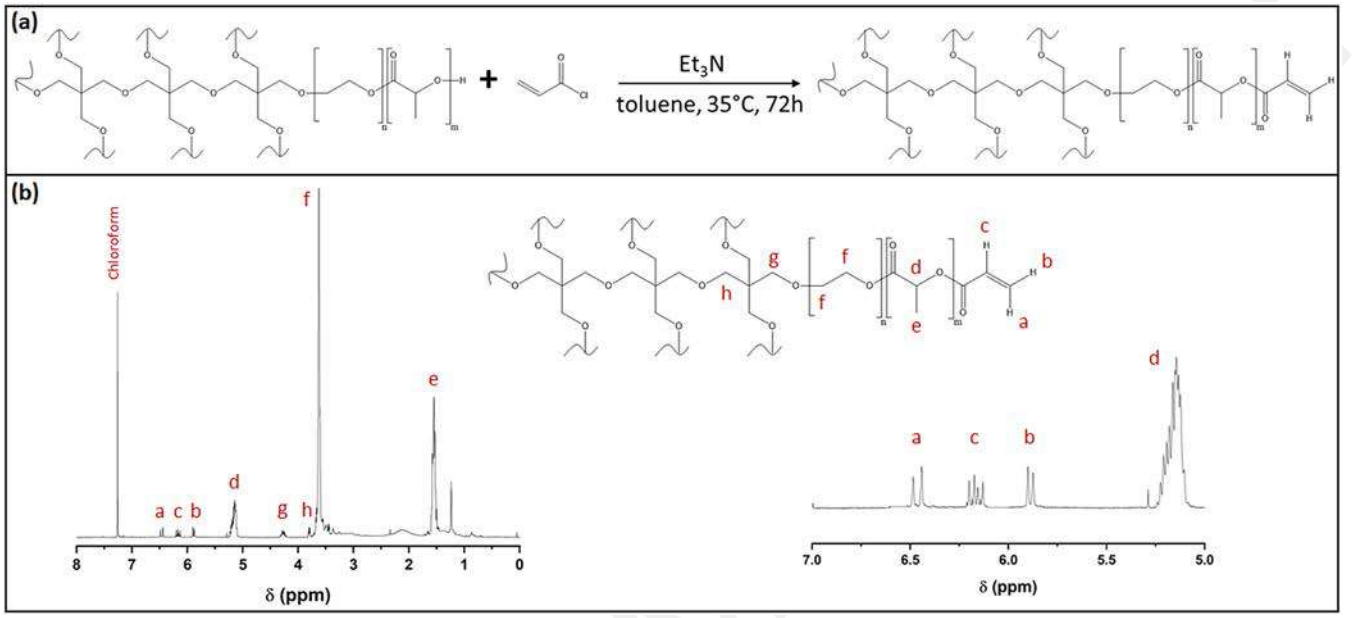

Figure 2. Structure and ^{1}H NMR ($CDCl_3$, 400 MHz) of acrylate functional copolymer. (a) Synthetic pathway to yield acrylated star-shaped PEG_{s8}−PLA copolymers. (b) ^{1}H NMR analysis of PEG_{8arm}20k−$(PLA_{13})_8$−AC with full (left) and zoomed (right) spectra.

specimen on a surface of 10 × 10 mm^2 before being covered by a second specimen (Figure 6b), and the formed excess was removed. AC-Gel and MC-Gel were applied between the sections (10 × 2 mm^2) of two specimens (Figure 6c) before being exposed to UV light for 5 min with a Dymax QX4 system (LEDs irradiating at 365, 385, and 405 nm). The distance measured between LEDs and samples was 3 cm. After 10 min, the adhesive properties were assessed on a MTS Systems Corporation machine equipped with a 25N load cell. The tests were performed at a constant rate of 15 mm·min^{-1}. The maximal force of detachment between substrates was recorded, and the corresponding adhesive strength was calculated by normalizing with respect to the area.

2.6. Degradation Study. The chemically cross-linked gels were dried before being weighed (Wi = initial weight), immersed in 5 mL of phosphate buffered saline (PBS) (pH 7.4), and placed at 37 °C under stirring. At different time points, the gels were removed from PBS and dried to constant mass (Wx = dry weight after x time in PBS). The remaining mass of the samples was calculated from eq 2.

$$\text{remaining mass (\%)} = \frac{Wx}{Wi} \times 100 \quad (2)$$

2.7. Cytotoxicity Assay. Cells and control polymer films were chosen following ISO 10993-5 guidelines. Mouse fibroblast L929 cells (ECACC 85011425) were maintained in DMEM high glucose supplemented with 5% Fetal Bovine Serum (FBS), 1% L-glutamine, and 1% penicillin/streptomycin and cultured at 37 °C and 5% CO_2. Cells were tested to be free of mycoplasms. Negative (RM-C High Density Polyethylene noted C−) and positive (RM-B 0.25% Zinc DiButyldithioCarbamate (ZDBC) polyurethane, noted C+) control films were purchased from Hatano Research Institute (Ochiai 729-5, Hadanoshi, Kanagawa 257, Japan). Cytotoxicity was assessed on extracts. Extractions were carried out on 100 mg of polymer gel per mL for 24 h at 37 °C under sterile conditions in complete growth medium, following ISO 10993-12 recommendations. Samples were irradiated under UV light for 5 min for decontamination. L929 cells were seeded at 10 × 10^3 cells per well in a 96-well plate and allowed to attach overnight. The culture medium was then removed and discarded from the cultures, and an aliquot of the film extract was added into each well. After 24 h of incubation under an appropriate atmosphere, extract cytotoxicity was assessed. The CellTiter-Glo Luminescent Cell Viability Assay was used for MC-Gel and AC-Gel, according to the manufacturer's instruction. Briefly, 50 μL of medium from each well was removed, following by the addition of the same volume of CellTiter-Glo. After 10 min of incubation at room temperature, luminescence was measured using a CLARIOstar microplate-reader (BMG LABTECH's) to quantify the ATP present. For CT-Gel, as the polymer was soluble in the culture medium and colored, a Crystal Violet Assay was used. In short, the medium from each well was removed and cells were washed with PBS twice. Cells were then fixed with paraformaldehyde solution at 3.7% (50 μL/well). After 10 min, the paraformaldehyde was removed before washing the cells with PBS. Crystal Violet staining solution at 0.1% was added (100 μL/well). After 30 min, cells were washed with distilled water three times followed by the addition of 200 μL of the acetic acid solubilization solution (10%). The absorbance at 595 nm was measured using a CLARIOstar microplate-reader (BMG LABTECH's).

3. RESULTS AND DISCUSSION

As explained in the introduction, we chose to work with star-shaped PEG−PLA block copolymer to try to overcome the issues encountered by existing commercial bioadhesives. By tuning the ratio between ethylene glycol and lactic acid units, it

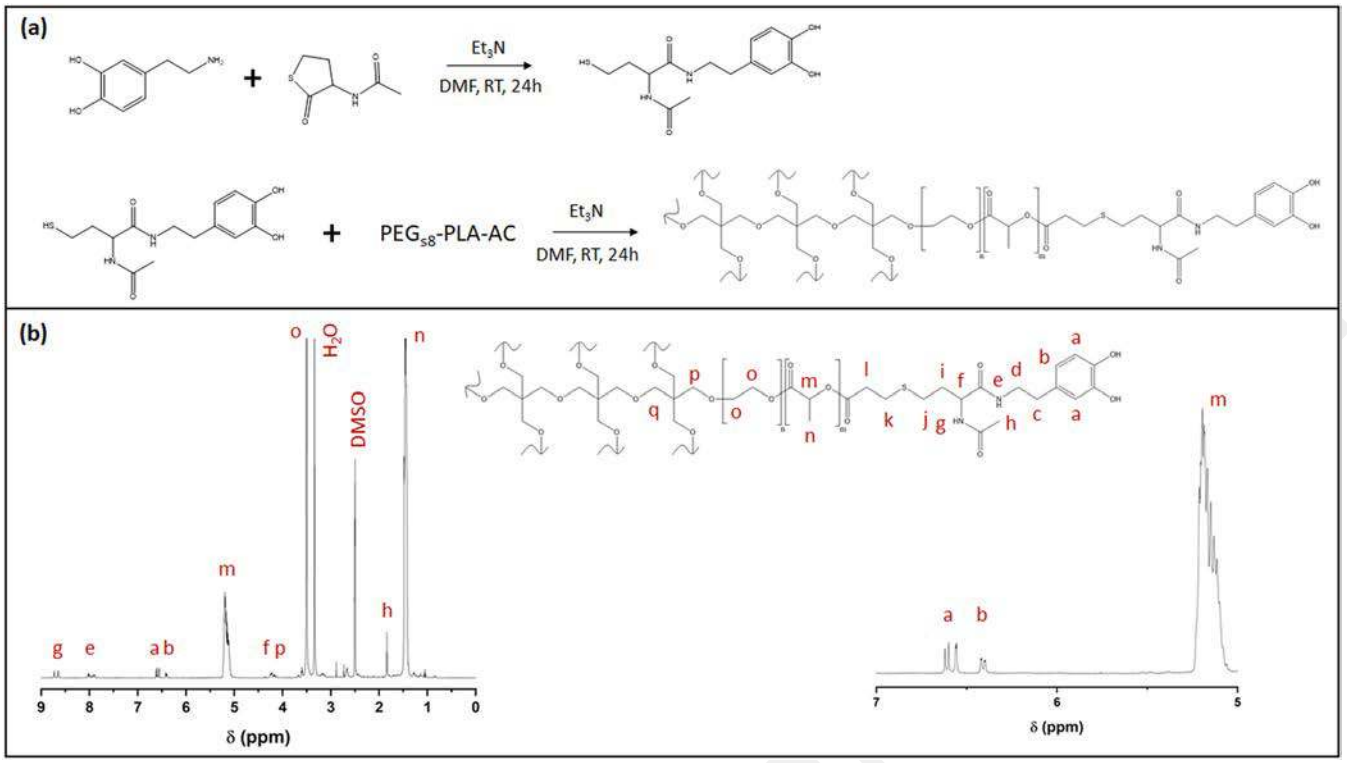

Figure 3. Structure and ^{1}H NMR (DMSO-d_6, 400 MHz) of catechol functional copolymer. (a) Synthetic pathway to yield catechol-functional star-shaped PEG_{s8}−PLA copolymers. (b) ^{1}H NMR analysis of $PEG_{8arm}20k$−$(PLA_{13})_8$−CT with full (left) and zoomed (right) spectra.

is possible to obtain water-soluble polymers that form hydrogels with stronger mechanical properties compared to linear counterparts.[28−30] Moreover, 8-armed copolymers were selected to increase the number of reactive sites per molecule and allow the formation of networks. Finally, by functionalizing the chain-ends with different types of moieties, different bioadhesive systems could be developed.

3.1. Synthesis of the Copolymers. First, PEG_{s8}−PLA was synthesized by classical ROP procedures already described by our group.[34] The molecular weight calculated by ^{1}H NMR agreed with the targeted molecular weight, and a low dispersity of 1.1 was confirmed by SEC analyses (Table 1).

Then, with the aim to design photocurable bioadhesive gels based on physical entanglement and interlocking, the non-functional star-shaped block copolymer PEG_{s8}−PLA was reacted with methacryloyl chloride or acryloyl chloride to yield multi(methacylate) star-shaped PEG_{s8}−PLA−MC[34] (Figure S2) and multi(acrylate) star-shaped PEG_{s8}−PLA−AC (Figure 2a).

The experimental molecular weights, the monomodal distributions, and unchanged dispersities ($Đ$ = 1.1) highlighted that no degradation of the copolymers occurred during this functionalization step (Table 1). A typical ^{1}H NMR spectrum of methacrylate functional 8-armed star-shaped PEG−PLA copolymer is shown in Figure S2. Peaks at 6.2 and 5.6 ppm (peaks a and b) and the peak at 1.8 ppm (peak c) correspond to alkene and methyl protons of the methacrylate chain-ends, respectively. The peaks at 5.1 ppm (peak d) and 1.5 ppm (peak e) correspond to the methine and methylene groups of the PLA backbone, respectively. The peaks at 4.3 ppm (peak g) were attributed to both the tripentaerythritol core and the (OH)-terminal of the copolymers. Finally, the peak at 3.6 ppm (peak f) was assigned to the methylene groups of PEG. By comparison between the integration of the peaks of the methylene groups of PEG and of the methacrylate chain-ends, a functionalization degree of 100% was calculated. The grafting of methacrylate functions onto star-shaped PEG−PLA chain-ends was further confirmed by ^{1}H DOSY NMR since methacrylate and copolymer signals had the same coefficient of diffusion (Figure S3). A typical ^{1}H NMR spectrum of PEG_{s8}−PLA−AC is shown in Figure 2b. Peaks at 6.4, 6.1, and 5.8 ppm (peaks a, c, and b) correspond to alkene protons of the acrylate chain-ends. The other peaks correspond to the star-shaped PEG_{s8}−PLA as described previously. By comparison between the integration of the peaks of the methylene groups of PEG and of the acrylate chain-ends, a functionalization degree of 100% was calculated. Again, the grafting of acrylate functions onto star-shaped PEG−PLA chain-ends was further confirmed by ^{1}H DOSY NMR since acrylate and copolymer signals had the same coefficient of diffusion (Figure S4).

In a second approach, catechol moieties were selected to obtain gels that can display adhesive properties thanks to hydrogen bonds but also covalent ones with functional groups of living tissues after oxidation. To this end, dopamine hydrochloride was reacted with citiolone to form a catechol-thiol intermediate. Then, a Michael addition reaction was carried out with PEG_{s8}−PLA−AC to obtain multi(catechol) star-shaped PEG_{s8}−PLA−CT (Figure 3a). The molecular weight determined by ^{1}H NMR agreed with the targeted one (Table 1). A typical ^{1}H NMR spectrum of PEG_{s8}−PLA−CT is shown Figure 3b. Peaks at 6.6 and 6.4 ppm (peaks a and b) correspond to aromatic protons of the catechol chain-ends. The peaks at 1.8 and 8.8 ppm (peaks g and h) correspond to the CH_3 and NH of the acetamide group, respectively. The peak at 8.1 ppm (peak e) was attributed to the amine proton

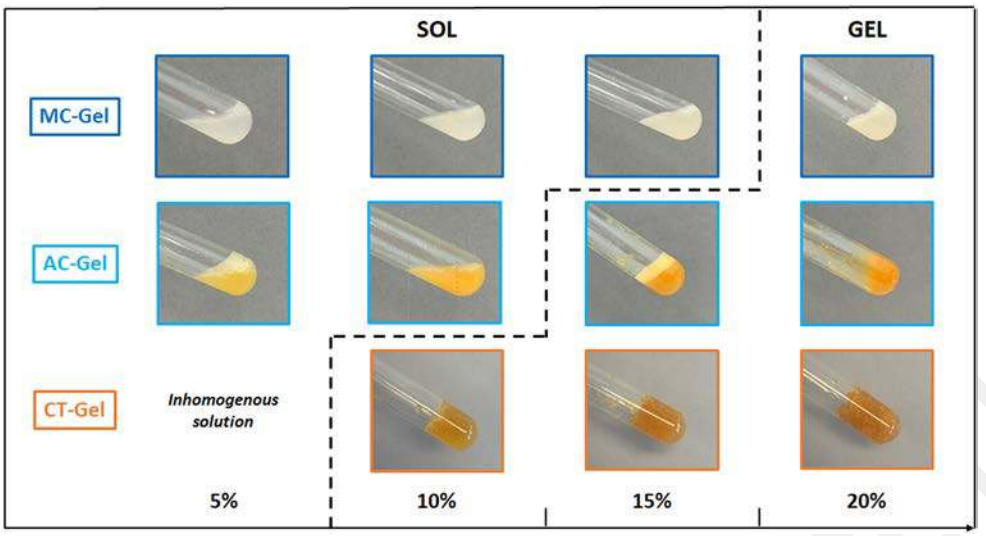

Figure 4. Visual aspect of the aqueous formulations of bioadhesive copolymers. Pictures of solutions or hydrogels obtained by mixing PEG_{s8}–PLA–MC (top row), PEG_{s8}–PLA–AC (middle row), or PEG_{s8}–PLA–CT (bottom row) in water at different concentrations (5, 10, 15, or 20 wt %).

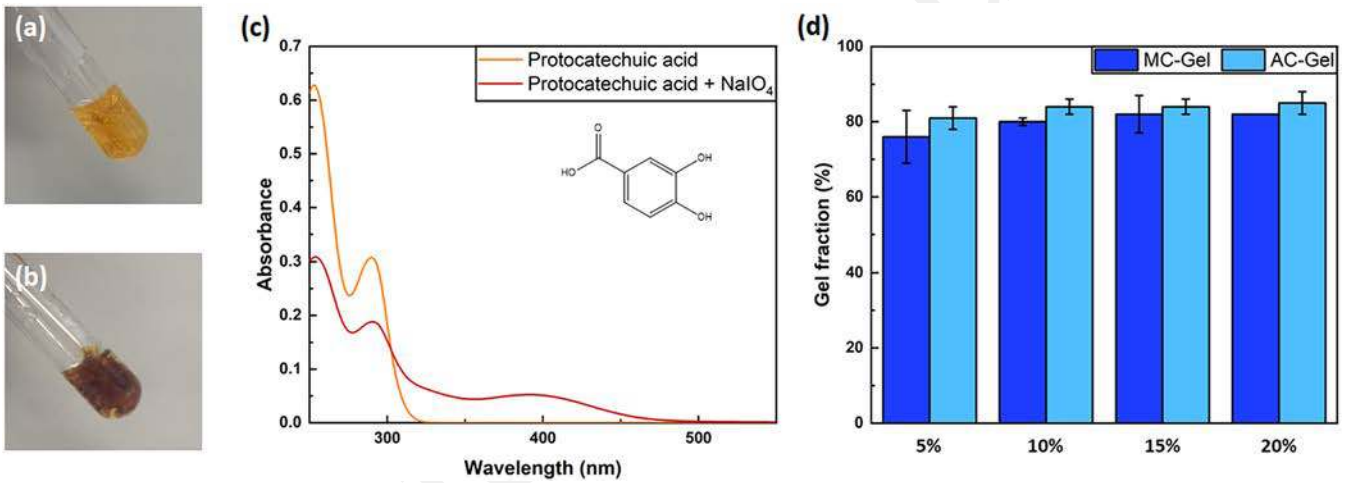

Figure 5. Characterizations of the physical and chemical bioadhesive hydrogels. (a–c) Highlighting the oxidation of PEG_{s8}–PLA–CT hydrogels by $NaIO_4$ with (a) CT-Gel; (b) oxidized CT_{OX}-Gel. (c) UV–vis spectra of protocatechuic acid with and without the presence of $NaIO_4$. (d) Gel fraction of the acrylate and methacrylate hydrogels after UV irradiation at different concentrations (wt %). Data are expressed as means ± SD and correspond to measurements with $n = 3$.

coming from the dopamine molecule. The other peaks correspond to the star-shaped PEG_{s8}–PLA as described previously. By comparison between the integration of the peaks of the methylene groups of PEG and of the aromatic catechol chain-ends, a functionalization degree of 100% was calculated. The grafting of catechol functions was further confirmed by the disappearance of the peaks corresponding to the acrylate groups but also by ^{1}H DOSY NMR (Figure S5). Moreover, the appearance of a characteristic catechol UV signal (290 nm) in SEC analysis, not present in PEG_{s8}–PLA–AC, further confirmed the success of the grafting.

These results confirmed the successful chain-end functionalization of star-shaped PEG_{s8}–PLA with methacrylate, acrylate, and catechol moieties that will allow the preparation of different types of bioadhesive hydrogels.

3.2. Preparation of the Gels. The synthesized polymers were then used to design hydrogels. Depending on the nature of the copolymer, different types of gels could be obtained. Physical CT-Gels were simply prepared by mixing PEG_{s8}–PLA–CT with water at the right concentration. Adding $NaIO_4$ solution allowed the oxidization of the catechol moieties to quinone,[32,37] leading to CT_{OX}-Gels. On the other hand, in order to be formed, photo-cross-linked AC-Gels and MC-Gels were required to be exposed to UV light after dissolution of PEG_{s8}–PLA–AC or PEG_{s8}–PLA–MC in water.

In any case, the first step that consisted of preparing an aqueous solution of the copolymers by mixing them with water was carefully carried out for several reasons. First, the concentration of polymer in water is a critical parameter for the formation of gels, especially for physical ones (CT-Gels). Then, even if several concentrations could lead to the formation of gels, the aspect and texture, and more specifically the viscosity, of the resulting mixture that would be applied on the injured tissue could impact the adhesive properties. It is important to find the best compromise between the amount of polymer, which would be responsible for the creation of the

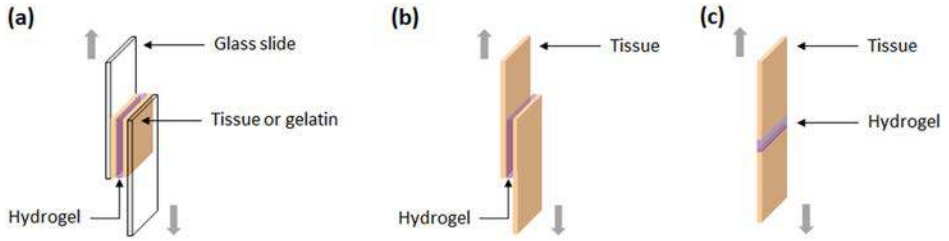

Figure 6. Mechanical testing methods used to evaluate the adhesive properties of the formulations: (a) Lap-shear test on coated glass slides (contact area: 25 × 25 mm^2). (b) Lap-shear test on tissue (contact area: 5 × 5 mm^2 for mouse skin, 10 × 10 mm^2 for human cadaveric colonic tissue). (c) Tensile test on tissue (contact area: 10 × 1 mm^2 for mouse skin, 10 × 2 mm^2 for human cadaveric colonic tissue).

network between the adhesive and the tissue thanks to its reactive moieties, and water that enables the interpenetration in the tissue. Indeed, the tissue penetration is a significant parameter in the bioadhesion field, and it is driven by polymer diffusion that could be affected by concentration, hydrophilicity, or hydrophobicity.[38] Therefore, PEG_{s8}−PLA−CT, PEG_{s8}−PLA−AC, and PEG_{s8}−PLA−MC were mixed in water at four different concentrations (5, 10, 15, and 20 wt %) to study the influence of the concentration on the gel formation and later on the adhesive properties. The resulting mixtures are shown in Figure 4, and their viscosity values are presented in Table S1.

We first investigated the formation of physical CT-Gels with PEG_{s8}−PLA−CT by using the vial tilting method. Gels could be obtained at concentrations of 10, 15, and 20 wt %, whereas the mixture remained at the liquid state for a concentration of 5%. As expected, increasing the concentration led to stiffer hydrogels. The viscosity increased from 5.3 Pa·s for a gel at 10 wt % to 70.3 Pa·s for a gel at 20 wt %. CT-Gels at 10, 15, and 20 wt % were thus selected for adhesion testing to evaluate the impact of the water/polymer ratio on the adhesive properties resulting from hydrogen bonds between catechol moieties and functional groups of tissues (e.g., amine, thiol, alcohol, carboxylic acid).

These hydrogels were oxidized by the addition of $NaIO_4$ to change the catechol functions to quinone groups and able to create covalent linkages through Michael addition and Schiff base reaction with amines, thiols, and imidazoles of living tissues. Of note, we chose to work with $NaIO_4$, which is a well-known fast and efficient chemical oxidizer. Its use allowed us to easily oxidize our polymers in order to demonstrate the adhesive properties of quinone-based hydrogels. However, because of its toxicity, $NaIO_4$ could hardly be in contact with patients and should be replaced by another oxidant system, such as horseradish peroxidase/hydrogen peroxide or mushroom tyrosinase/oxygen.[39−42]

The oxidation of catechol moieties by $NaIO_4$ was first detected by the change of color of the samples (Figure 5a,b). Indeed, CT-Gels displayed an orange color whereas CT_{OX}-Gels turned brown. The phenomenon was confirmed using UV−vis spectroscopy as shown in Figure 5c. As described in the literature,[39,43] in the presence of $NaIO_4$, the catechol group from protocatechuic acid is oxidized to quinone, resulting in the decrease of intensity of the peak at 290 nm and the appearance of a new peak at 400 nm. Of note, to check that the initial properties of the physical CT-Gels were not affected by oxidation in water, we also evaluated the extent of oxidation of CT-Gel solutions in PBS at pH 7.4 and in water at pH 8 by UV−vis spectroscopy. No peak at 400 nm was detected which confirms that no oxidation occurred under these conditions (data not shown).

Then, photocurable hydrogels were prepared using PEG_{s8}−PLA−AC and PEG_{s8}−PLA−MC. As described previously, the polymers were first dissolved in water at different concentrations. For PEG_{s8}−PLA−MC, the mixtures stayed in a liquid state between 5 and 15 wt % and formed a gel at 20 wt % because of increased interactions between hydrophobic PLA blocks.[44] PEG_{s8}−PLA−AC behaved differently since it remained in a liquid state at 5 and 10 wt % but became a gel at 15 and 20 wt %. The viscosity increased with the concentration, from 4.6 × 10^{-3} to 1.4 Pa·s for PEG_{s8}−PLA−MC and from 9.2 × 10^{-3} to 4.9 Pa·s for PEG_{s8}−PLA−AC. These differences could have an impact on the adhesive properties investigated in the next part of this work. In a second step, the mixtures were irradiated under UV light to yield photo-cross-linked AC-Gels and MC-Gels. Whatever the initial concentration, cured gels were obtained. In order to confirm the creation of 3D networks after UV irradiation and evaluate the chemical cross-linking, gel fractions were measured. All samples exhibited gel fractions around 80% (Figure 5d), which confirmed the cross-linking efficiency of the star-shaped copolymers without the need to use photoinitiators that may be toxic in the frame of the application. The gel fraction slightly increased with the concentration, which can be explained by the increased proximity of polymer chains and reactive moieties for higher concentrations. Moreover, in agreement with the higher reactivity of acrylate groups compared to methacrylate ones, AC-Gels exhibited slightly higher gel fractions than MC-Gels at equal concentrations.

3.3. Adhesive Properties. The impact of different parameters on the adhesive properties has been investigated. First, gels with different adhesion mechanisms like physical bonds (CT-Gel), chemical covalent linkages (CT_{OX}-Gel), or the creation of an interweaved network between polymer and tissue (AC-Gel and MC-Gel) were explored and compared (Figure 1). Then, different concentrations of gel were tested to evaluate the impact of the polymer/water ratio. It is expected that the quantity of polymer influences the creation of the network between adhesive and tissue as a function of the number of functional groups present, whereas the quantity of water influences the ease of diffusion and interpenetration in the tissue. An optimum between these two factors to yield appropriate adhesion properties should therefore be found. Finally, the impact of the variation of reactivity between two photoreactive moieties was investigated (AC-Gel and MC-Gel). nF-Gel, prepared with nonfunctional PEG_{s8}−PLA, was used as a reference to confirm that the adhesive properties were brought by the different functional moieties of the functional star-shaped copolymers and not by the diffusion and

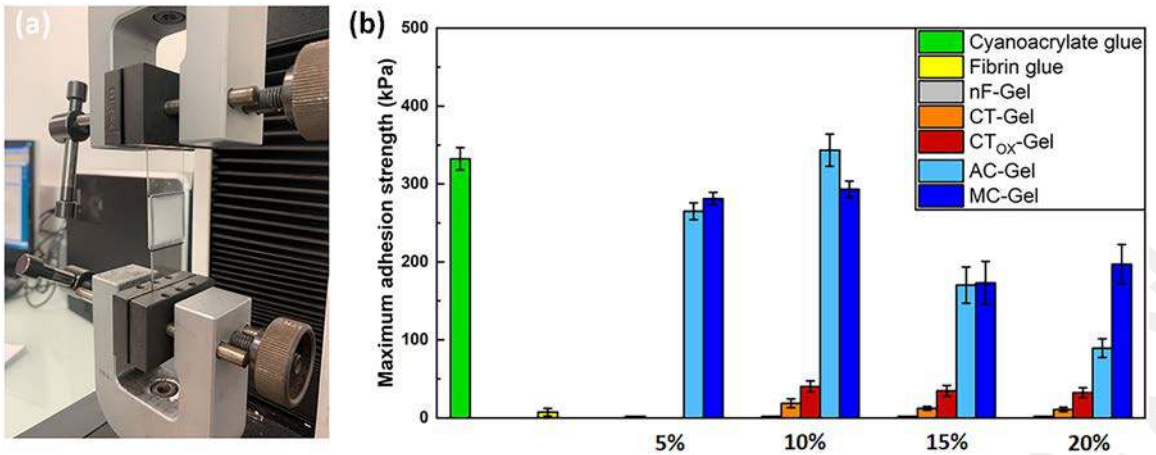

Figure 7. Evaluation of the adhesion on gelatin model substrate. (a) Illustration of the lap-shear test on gelatin coated glass slides (contact area: 25 × 25 mm^2). (b) Maximum adhesion strength on gelatin coating measured for the various gels and references. Data are expressed as means ± SD and correspond to measurement with n = 3.

interpenetration of the nonfunctional PEG−PLA segments. In order to compare the properties of the developed hydrogels with existing commercial adhesives, Tisseel fibrin glue and Leukosan adhesive cyanoacrylate glue were also tested in the same conditions.

The adhesive properties of the different systems were preliminarily tested on gelatin coating. This simple technique allowed one to easily screen the numerous samples and select the most promising ones. The gelatin model was chosen since it is a widespread model in the field of bioadhesion.[15,35,45−48] It presents a large number of amino groups in its composition and therefore can simulate the composition of living tissues.[15,36,47,49,50] The bioadhesion of CT-Gel and CT_{OX}-Gel at 10, 15, and 20 wt % and AC-Gel and MC-Gel at 5, 10, 15, and 20 wt % was evaluated through a lap-shear test (Figure 6a). CT-Gels and CT_{OX}-Gels, as well as references, were applied in the overlap area of two gelatin coated glass slides and tested after 15 min. AC-Gels and MC-Gels were exposed to UV light for 5 min after being applied between the slides and then tested after 10 min of rest. The maximal force of detachment between substrates was recorded, and the corresponding adhesive strength was calculated by normalizing with respect to the contact area.

All the hydrogels made of polymers modified with functional groups at their chain-ends displayed increased adhesive strength compared to nF-Gel, for which the values ranged from 0.1 ± 0.1 to 0.3 ± 0.1 kPa only. This confirmed that the selected functional groups were able to interact with gelatin and yield adhesive properties. Depending on the type of functionalization and therefore on the mechanism involved in the adhesion, the gels displayed distinctive behaviors. The results are presented in Figure 7b and Table S1. According to these results, samples could be classified into two categories: the catechol-based systems (CT-Gel and CT_{OX}-Gel) with lower values of adhesion strength on the one hand and the photo-cross-linkable systems (AC-Gel and MC-Gel) with higher values on the other hand. Not surprisingly, CT-Gel for which the adhesion was only due to hydrogen bonds exhibited the lower adhesive strength with values between 10.7 ± 2.7 and 18.6 ± 5.6 kPa. The oxidized counterpart CT_{OX}-Gel displayed increased values from 32.3 ± 6.4 to 40.2 ± 7.3 kPa since it could form covalent linkages with the gelatin in addition to hydrogen bonding. Of note, although the ability of oxidized catechols to bind covalently could increase with time,[51] we evaluated the adhesion of CT_{OX}-Gel under the same conditions as the other ones in order to compare the systems and evaluated the initial adhesion strength. Significantly better results were obtained with AC-Gel and MC-Gel. For AC-Gel, the maximum adhesion strength reached 343.3 ± 20.6 kPa against 293.2 ± 10.6 kPa for MC-Gel. The difference can be explained by the higher reactivity of acrylate compared to methacrylate and is in accordance with the gel fractions measured previously. These results also confirmed that creating an interpenetrated network between polymer and tissue through interlocking and entanglement upon photopolymerization is an effective method to reach strong adhesion.

Among all the different types of hydrogels and whatever the mechanism of adhesion involved, the concentration of 10 wt % always led to the best results. This concentration appeared to be the best compromise between the quantity of water and polymer to ensure both a good interpenetration of the adhesive preparation in the tissue and the creation of a network between the functional polymer and the substrate.

In comparison with commercial cyanoacrylate and fibrin glues, the designed bioadhesive formulations showed interesting adhesive properties with MC-Gel and AC-Gel exhibiting adhesion strength similar to cyanoacrylate (332.4 ± 14.5 kPa), whereas CT-Gel and CT_{OX}-Gel displayed higher adhesion strength than fibrin glue (7.2 ± 4.9 kPa).

Based on the results obtained on gelatin coating, mouse skin was then chosen as a biological substrate for further investigations on CT-Gel, CT_{OX}-Gel, AC-Gel, and MC-Gel at 10 wt %. Although we are aware that crack initiation and boundary effects are important matters for adhesion[3] as a result of tissue irregularities and that it is impossible to UV-cure the (meth)acrylate-based systems through the tissues, two testing methods were used as a function of the nature of the adhesive. A lap-shear test was used to evaluate CT-Gel, CT_{OX}-Gel, cyanoacrylate, and fibrin glues (Figure 6b). MC-Gel and AC-Gel were tested through tensile test (Figure 6c) to allow for their irradiation under UV light. In both cases, the tests were carried out 15 min after the application between the skin specimens. Of note, lower adhesion of the gels on mouse skin compared to the gelatin model was observed for all samples, including the commercial glues. In more details, like for gelatin, 10 wt % AC-Gel and MC-Gel showed better results on mouse

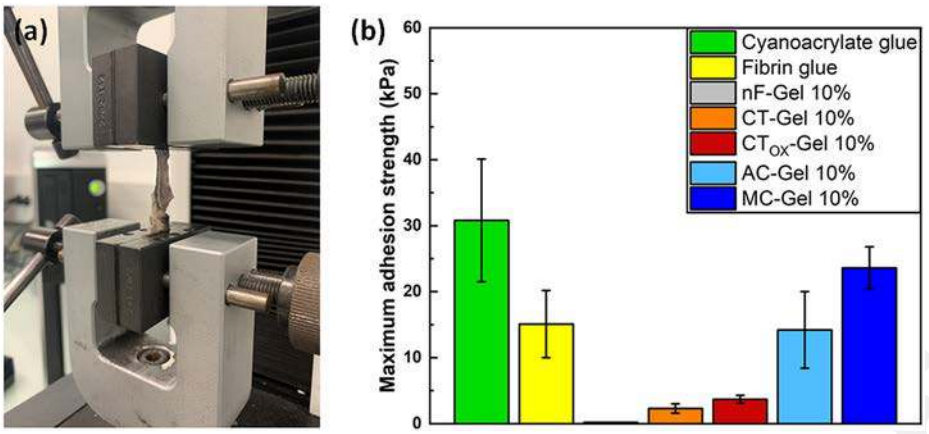

Figure 8. Evaluation of the adhesion on mouse skin. (a) Illustration of the lap-shear test with mouse skin. (b) Maximum adhesion strength on mouse skin of the various designed gels and references (lap-shear for CT-Gel, CT_{OX}-Gel, cyanoacrylate, and fibrin glues with contact area: 5 × 5 mm^2; tensile test for MC-Gel and AC-Gel with contact area: 10 × 1 mm^2). Data are expressed as means ± SD and correspond to measurements with n = 3.

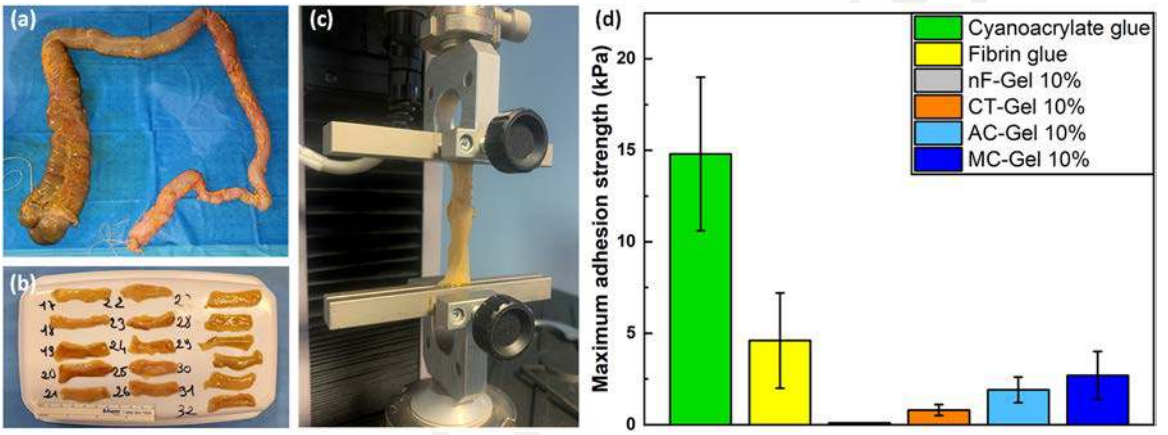

Figure 9. Evaluation of the adhesion on human cadaveric colon. (a) Colon after collection. (b) Colonic samples after cutting (50 × 10 mm). (c) Picture of adhesion testing on colonic samples. (d) Maximum adhesion strength on colonic samples of the various designed gels and references (lap-shear for CT-Gel, cyanoacrylate, and fibrin glues with contact area: 10 × 10 mm^2; tensile test for MC-Gel and AC-Gel with contact area: 10 × 2 mm^2). Data are expressed as means ± SD and correspond to measurements with n = 3.

skin compared to the catechol-based adhesives (Figure 8). AC-Gel displayed adhesive properties similar to commercial fibrin glue with values of 14.2 ± 5.8 and 15.1 ± 5.1 kPa, respectively. For MC-Gel, the maximum adhesion strength reached 23.6 ± 3.2 kPa, which was higher compared to fibrin and close to cyanoacrylate (30.8 ± 9.3 kPa). Coming to the catechol-based hydrogels, even if CT-Gel (2.3 ± 0.7 kPa) and CT_{OX}-Gel (3.7 ± 0.6 kPa) exhibited lower values, the adhesion strength remained higher than the reference nF-Gel for which the samples could not support their own weight after application of the formulation.

Finally, the adhesive properties were evaluated on human cadaveric colonic tissue (Figure 9). Due to the low adhesion obtained on mouse skin and the safety concerns with $NaIO_4$, CT_{OX}-Gel was not investigated with this new tissue. The study focused only on CT-Gel, AC-Gel, and MC-Gel at 10%. As described before, CT-Gel and commercial references were tested through lap-shear tests (Figure 6b), whereas tensile tests (Figure 6c) were used for AC-Gel and MC-Gel. Again, CT-Gel, AC-Gel, and MC-Gel exhibited higher adhesion strength compared to the reference nF-Gel, which confirmed the benefit of functionalizing the chain-ends of the copolymer with various groups to confer bioadhesion abilities. Indeed, after application of nF-Gel between two colonic specimens, the samples were not able to support their own weight and immediately fell apart when lifted. Moreover, a similar trend to what has been demonstrated before was observed between the different gels. CT-Gel displayed the lowest value of adhesive strength (0.8 ± 0.3 kPa), whereas photo-cross-linkable AC-Gel and MC-Gel showed better results, with values of 1.9 ± 0.7 and 2.7 ± 1.3 kPa, respectively.

In this case, the designed bioadhesives showed reduced properties compared to commercial ones (4.6 ± 2.6 kPa for fibrin and 14.8 ± 4.2 kPa for cyanoacrylate glue), but it is important to notice that the colon is hardly studied in the field of bioadhesion. The results could be explained by the nature of the substrate. Indeed, colonic tissue is covered with mucus that can interfere with the mechanism responsible for bioadhesive properties. Moreover, colon specimens were highly hydrated, which can impact the adhesive properties negatively. Indeed, Michel et al. demonstrated that the performance of adhesion can be governed by the fluid transport across the interface between tissue and hydrogel and more precisely that adhesion depends on a competition between draining and wetting of the interface.[25] Finally, the experiments were not performed on fresh colonic tissue, and the softness of the samples made them

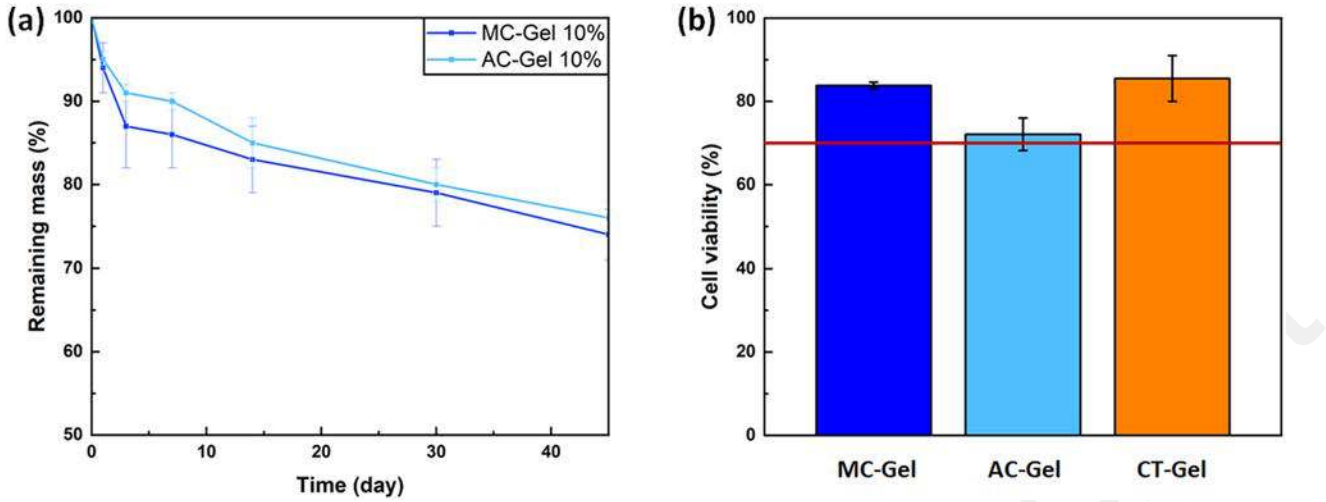

Figure 10. (a) Evaluation of the degradation of photo-cross-linked samples in PBS (pH 7.4) at 37 °C. (b) Cell viability evaluation assessed on L929 cells after treatment with the extract of gels for 24 h. Data are expressed as means ± SD and correspond to measurements with $n = 3$.

difficult to handle. Therefore, the results may not be representative of what might be observed in the body. It should also be noted that even the commercial glues led to very low adhesion strength of <15 kPa.

As demonstrated, the substrate on which the tests were carried out had an important influence on the results. Therefore, it is difficult to compare precisely our study to what is already described in the literature. However, our results are still within the range, if not better, compared to data of the literature. For instance, Assmann et al. displayed adhesive strengths ranging from 5 to 300 kPa for their system based on gelatin methacryloyl, when tested on gelatin.[35] These results are similar to those obtained with AC-Gel and MC-Gel. Systems based on oxidized catechol moieties were designed by Cencer et al. and exhibited adhesive strength of 8 kPa on bovine pericardium,[43] which is close to what was obtained for CT_{OX}-Gel on mouse skin in our case. Another example referred to adhesive hydrogel containing PEG diacrylate, in association with maleic anhydride modified chitosan and benzaldehyde-terminated PEG.[46] In this case, the adhesive properties were tested on a hybrid system composed of porcine skin and gelatin, and adhesion strength values between 26 and 47 kPa were reported. As a last example, catechol−PEG−PCL constructs exhibited maximum adhesive strengths on bovine pericardium ranging from 9 to 45 kPa after oxidation with $NaIO_4$.[24]

To conclude on the adhesion tests, this set of results demonstrated the potential of the designed star-shaped PEG−PLA hydrogels to be used as bioadhesives for soft tissue applications. Depending on the chain-end functionalization (CT versus MC or AC) but also on the nature of the substrate, the gels exhibited various adhesive capacities that are in most cases comparable to the ones of commercial glues. One hypothesis to explain the results obtained on mouse skin and human cadaveric colonic tissue is that the optimum concentration of gels could be different depending on the substrate. Therefore, to go further, it would be interesting to also assess the adhesive properties of the gels at various concentrations on the biological substrates. The study of the evolution of the adhesion strength as a function of time would also be useful to target the final application more precisely. Indeed, it is possible that some systems need a longer time to form a robust adhesion, such as CT_{OX}-Gels that need to react with the functional groups of tissues to bind covalently.[51] Finally, to better understand the different behaviors, the mechanical properties of the hydrogels and their ability to dissipate mechanical energy should also be evaluated.[3] Indeed, even if the impact of the mechanical properties of the adhesives is often overlooked, designing bioadhesives with mechanical properties matching those of the tissues allows optimal performances to be reached. When the adhesives are too rigid compared to the biological tissues to which they are bonded, the mechanical stress is concentrated at the interface between tissue and adhesive and this stress concentration can lead to the mechanical failure of adhesion or delamination. Moreover, the ability of bioadhesives to dissipate stress is also an important parameter to prevent cohesive failure and can be improved by tuning the viscoelastic properties of the adhesives. Viscoelastic materials, unlike elastic materials, can dissipate energy and therefore relieve the mechanical resistance to deformation over time. An interesting technique to prepare adhesive matrices able to dissipate applied stresses is to design polymeric adhesives based on a double network, one with strong cross-linking and the other with weak cross-linking providing sacrificial bonds to prevent crack propagation. In this perspective, adhesives based on hybrid stars with both methacrylate and catechol functions on a same star were initially designed. Preliminary tests were carried out with such hybrid systems, but the obtained adhesion properties were intermediate between CT-Gel and MC-Gel with higher adhesion with higher methacrylate content (see details in the Supporting Information). Since this strategy did not lead to a synergetic effect, it was not explored in the frame of the present work. However, this approach should be further studied for future developments by investigating the impact of the methacrylate/catechol ratio, for instance.

3.4. Degradation and Cytocompatibility. With the objective to use these hydrogels as temporary tissue adhesives, their degradation was investigated *in vitro*. The mass loss of AC-Gel and MC-Gel at 10% was monitored over 45 days when they were immersed in PBS at 37 °C (Figure 10a). As expected, after a short period of rapid mass loss, the samples exhibited linear mass loss, which is characteristic of degradable networks cross-linked chemically and prevents the materials

from the abrupt loss of properties. In more details, AC- and MC-Gels lost 10% to 15%, respectively, of their mass in the first 2 days due to the diffusion of the non-cross-linked chains, which is in accordance with the values obtained for gel fractions. After this initial period, the degradation rate was similar for both hydrogels with a slow and constant weight loss of 0.25% per day over the studied period. Of note, the copolymer used in this work to produce the MC-Gel bioadhesive was recently used to prepare elastomeric films via solvent evaporation and cross-linking. These dense networks were fully degraded after 100 days under the same *in vitro* conditions.[34]

Of note, the physically cross-linked hydrogels based on PEG_{s8}−PLA−CT could not be tested under these conditions since a large excess of water may solubilize them. Indeed, we demonstrated previously that at a concentration of 5% CT-Gel could not be formed and the mixture stayed in the liquid state. However, these gels are based on PEG−PLA copolymers known to be degradable and easily eliminated from the body. Indeed, PLA degrades into lactic acid by random scission of the ester linkages (hydrolysis), and the products of degradation can be metabolized or eliminated by renal excretion.[52,53] PEG below 20 000 $g{\cdot}mol^{-1}$ is bioeliminable by renal excretion.[54] Finally, it can be assumed that the degradation of CT_{OX}-Gel occurs slower compared to CT-Gel due to the creation of chemical bonds with the tissue.

Therefore, depending on whether the adhesive needs to stay for a long time or not on the injured tissue, the choice of the system could be adapted. AC-Gel and MC-Gel would be preferred for a long period, whereas CT-Gel would be favored for shorter times. Similarly, CT-Gel should not be used in wet environments and limited to skin applications since hydrogen bonds can be easily dissociated in the presence of excess water.[3] *In vivo* studies would also provide interesting information regarding the durability and the evolution of the viscosity of the gels since the environment in which the adhesives would be applied would have a strong impact on the performances. The composition also plays a critical role as demonstrated by a slow *in vivo* degradation of the commercial FocalSeal system composed of acrylated PEG−PLA and PEG−PTMC copolymers that resorb in 600 days, whereas the fully hydrophilic DuraSeal that contains only PEG and trilysine was reported to be resorbed in 8 weeks.[55,56]

Finally, the potential of the hydrogels to be used in contact with cells was assessed. The cytotoxicity of MC-Gel, AC-Gel, and CT-Gel at 10% was evaluated on extracts following ISO 10993-12 recommendations. The extracts from hydrogels or reference material C− and C+ were added on L929 fibroblasts seeded into wells, and cell viability was evaluated over a 24 h period (Figure 10b). Only extracts from positive control films (C+) gave 0% of cell viability on L929 cells. The extracts from MC-Gel, AC-Gel, and CT-Gel led to viability above 70% with values of 84%, 72%, and 86%, respectively. These results confirm the absence of acute cytotoxicity of the samples, which is a prerequisite for their use as bioadhesives.

4. CONCLUSION

In this work, we designed degradable bioadhesives based on PEG−PLA star-shaped hydrogels. By functionalizing the chain-ends with various moieties (acrylate, methacrylate, and catechol), different systems were investigated and their adhesive properties on gelatin, mouse skin, and human cadaveric colonic tissue were compared to those of commercial fibrin and cyanoacrylate references. Acrylate- and methacrylate-based hydrogels at 10 wt % exhibited adhesion strength (343 and 293 kPa, respectively) similar to cyanoacrylate (332 kPa) on gelatin coating, whereas catechol systems displayed higher values (11 and 19 kPa) compared to fibrin glue (7 kPa). Regarding biological substrates, colonic tissue appeared to be challenging, but the results obtained on mouse skin confirmed the potential of the 10 wt % acrylate and methacrylate gels that showed adhesion strength similar to fibrin glue for AC-Gels (around 15 kPa) and similar to cyanoacrylate for MC-Gels (around 25 kPa). Finally, the hydrolytic degradability and the absence of acute cytotoxicity were shown, which confirm their potential use as new bioadhesive systems.

ASSOCIATED CONTENT

Supporting Information

The Supporting Information is available at the end of the paper.

^{1}H NMR spectrum of star-shaped PEG−PLA copolymer; synthetic scheme of methacrylate functional copolymers and ^{1}H NMR spectrum of PEGs8-PLA-MC; ^{1}H DOSY NMR spectrum of the methacrylate functional PEG−PLA copolymer; ^{1}H DOSY NMR spectrum of the acrylate functional PEG−PLA copolymer; ^{1}H DOSY NMR spectrum of the catechol functional PEG−PLA copolymer; values of the viscosity (Pa·s) of solutions or hydrogels obtained by mixing PEGs8-PLA-MC, PEGs8-PLA-AC, and PEGs8-PLA-CT in water at different concentrations (5, 10, 15, and 20 wt %); preliminary study of the adhesion properties of bioadhesives based on hybrid methacrylate-catechol functional star-shaped PEG−PLA hydrogels (PDF)

AUTHOR INFORMATION

Corresponding Author

Benjamin Nottelet − *Polymers for Health and Biomaterials, IBMM, Univ Montpellier, CNRS, ENSCM, Montpellier 34095, France;* orcid.org/0000-0002-8577-9273; Email: benjamin.nottelet@umontpellier.fr

Authors

Mathilde Grosjean − *Polymers for Health and Biomaterials, IBMM, Univ Montpellier, CNRS, ENSCM, Montpellier 34095, France*

Edouard Girard − *Univ Grenoble Alpes, CNRS, CHU Grenoble Alpes, Grenoble INP, TIMC-IMAG, Grenoble 38058, France; Département de chirurgie digestive et de l'urgence, Centre Hospitalier Grenoble-Alpes, Grenoble 38043, France; Laboratoire d'anatomie des Alpes françaises (LADAF), UFR de médecine de Grenoble, Université Grenoble Alpes, Grenoble 38058, France*

Audrey Bethry − *Polymers for Health and Biomaterials, IBMM, Univ Montpellier, CNRS, ENSCM, Montpellier 34095, France*

Grégory Chagnon − *Univ Grenoble Alpes, CNRS, CHU Grenoble Alpes, Grenoble INP, TIMC-IMAG, Grenoble 38058, France;* orcid.org/0000-0002-9386-7046

Xavier Garric − *Polymers for Health and Biomaterials, IBMM, Univ Montpellier, CNRS, ENSCM, Montpellier 34095, France; Department of Pharmacy, Nîmes University Hospital, 30900 Nîmes, France*

Notes

The authors declare no competing financial interest.

ACKNOWLEDGMENTS

This work was supported by the ANR2019-OPENN held by the University of Montpellier (ANR-19-CE19-0022-02). The authors acknowledge Daniele Noël and Karine Toupet from the Institute for Regenerative Medicine and Biotherapy (IRMB) for the collection and donation of mouse skin. The authors thank Baptiste Jacquet and Nicolas Leprêtre for their experimental support for adhesion testing on human cadaveric colonic tissue (collection of the colons, sample cuttings). The authors also acknowledge the C3M team of the Institut Charles Gerhardt Montpellier (ICGM) for the access to the rheometer and Dimitri Berne for his help with the viscosity measurements.

REFERENCES

(1) Gurtner, G. C.; Werner, S.; Barrandon, Y.; Longaker, M. T. Wound Repair and Regeneration. *Nature* **2008**, *453*, 314−321.

(2) Annabi, N.; Tamayol, A.; Shin, S. R.; Ghaemmaghami, A. M.; Peppas, N. A.; Khademhosseini, A. Surgical Materials: Current Challenges and Nano-Enabled Solutions. *Nano Today* **2014**, *9*, 574−589.

(3) Nam, S.; Mooney, D. Polymeric Tissue Adhesives. *Chem. Rev.* **2021**, *121* (18), 11336−11384.

(4) Bao, Z.; Gao, M.; Sun, Y.; Nian, R.; Xian, M. The Recent Progress of Tissue Adhesives in Design Strategies, Adhesive Mechanism and Applications. *Mater. Sci. Eng., C* **2020**, *111*, 110796.

(5) Jain, R.; Wairkar, S. Recent Developments and Clinical Applications of Surgical Glues: An Overview. *Int. J. Biol. Macromol.* **2019**, *137*, 95−106.

(6) Bouten, P. J. M.; Zonjee, M.; Bender, J.; Yauw, S. T. K.; Van Goor, H.; Van Hest, J. C. M.; Hoogenboom, R. The Chemistry of Tissue Adhesive Materials. *Prog. Polym. Sci.* **2014**, *39*, 1375−1405.

(7) Korde, J. M.; Kandasubramanian, B. Biocompatible Alkyl Cyanoacrylates and Their Derivatives as Bio-Adhesives. *Biomater. Sci.* **2018**, *6*, 1691−1711.

(8) Xu, J.; Liu, Y.; Hsu, S. H. Hydrogels Based on Schiff Base Linkages for Biomedical Applications. *Molecules* **2019**, *24* (16), 3005.

(9) Lee, H. A.; Park, E.; Lee, H. Polydopamine and Its Derivative Surface Chemistry in Material Science: A Focused Review for Studies at KAIST. *Adv. Mater.* **2020**, *32*, 1907505.

(10) Sawhney, A. S.; Pathak, C. P.; van Rensburg, J. J.; Dunn, R. C.; Hubbell, J. A. Optimization of Photopolymerized Bioerodible Hydrogel Properties for Adhesion Prevention. *J. Biomed. Mater. Res.* **1994**, *28* (7), 831−838.

(11) Laulicht, B.; Mancini, A.; Geman, N.; Cho, D.; Estrellas, K.; Furtado, S.; Hopson, R.; Tripathi, A.; Mathiowitz, E. Bioinspired Bioadhesive Polymers: Dopa-Modified Poly(Acrylic Acid) Derivatives. *Macromol. Biosci.* **2012**, *12* (11), 1555−1565.

(12) Ito, T.; Otani, N.; Fujii, K.; Mori, K.; Eriguchi, M.; Koyama, Y. Bioadhesive and Biodissolvable Hydrogels Consisting of Water-Swellable Poly(Acrylic Acid)/Poly(Vinylpyrrolidone) Complexes. *J. Biomed. Mater. Res. - Part B Appl. Biomater.* **2020**, *108* (2), 503−512.

(13) Sawhney, A. S.; Pathak, C. P.; Hubbell, J. A. Bioerodible Hydrogels Based on Photopolymerized Poly(Ethylene Glycol)- Co-Poly(α-Hydroxy Acid) Diacrylate Macromers. *Macromolecules* **1993**, *26*, 581−587.

(14) Wallace, D. G.; Cruise, G. M.; Rhee, W. M.; Schroeder, J. A.; Prior, J. J.; Ju, J.; Maroney, M.; Duronio, J.; Ngo, M. H.; Estridge, T.; Coker, G. C. A Tissue Sealant Based on Reactive Multifunctional Polyethylene Glycol. *J. Biomed. Mater. Res.* **2001**, *58* (5), 545−555.

(15) Santos, J. M. C.; Marques, D. S.; Alves, P.; Correia, T. R.; Correia, I. J.; Baptista, C. M. S. G.; Ferreira, P. Synthesis, Functionalization and Characterization of UV-Curable Lactic Acid Based Oligomers to Be Used as Surgical Adhesives. *React. Funct. Polym.* **2015**, *94*, 43−54.

(16) Shagan, A.; Zhang, W.; Mehta, M.; Levi, S.; Kohane, D. S.; Mizrahi, B. Hot Glue Gun Releasing Biocompatible Tissue Adhesive. *Adv. Funct. Mater.* **2020**, *30* (18), 1900998.

(17) Ferreira, P.; Coelho, J. F. J.; Gil, M. H. Development of a New Photocrosslinkable Biodegradable Bioadhesive. *Int. J. Pharm.* **2008**, *352* (1−2), 172−181.

(18) Santos, J. M. C.; Travassos, D. R. S.; Ferreira, P.; Marques, D. S.; Gil, M. H.; Miguel, S. P.; Ribeiro, M. P.; Correia, I. J.; Baptista, C. M. S. G. Engineering Star-Shaped Lactic Acid Oligomers to Develop Novel Functional Adhesives. *J. Mater. Res.* **2018**, *33* (10), 1463−1474.

(19) Ferreira, P.; Silva, A. F. M.; Pinto, M. I.; Gil, M. H. Development of a Biodegradable Bioadhesive Containing Urethane Groups. *J. Mater. Sci. Mater. Med.* **2008**, *19* (1), 111−120.

(20) Zhang, W.; Ji, T.; Lyon, S.; Mehta, M.; Zheng, Y.; Deng, X.; Liu, A.; Shagan, A.; Mizrahi, B.; Kohane, D. S. Functionalized Multiarmed Polycaprolactones as Biocompatible Tissue Adhesives. *ACS Appl. Mater. Interfaces* **2020**, *12* (15), 17314−17320.

(21) Annabi, N.; Yue, K.; Tamayol, A.; Khademhosseini, A. Elastic Sealants for Surgical Applications. *Eur. J. Pharm. Biopharm.* **2015**, *95*, 27−39.

(22) Lee, S.-H.; Park, C.-W.; Lee, S.-G.; Kim, W.-K. Postoperative Cervical Cord Compression Induced by Hydrogel Dural Sealant (DuraSeal). *Korean J. Spine* **2013**, *10* (1), 44.

(23) Ferreira, P.; Coelho, J. F. J.; Gil, M. H. Development of a New Photocrosslinkable Biodegradable Bioadhesive. *Int. J. Pharm.* **2008**, *352* (1−2), 172−181.

(24) Murphy, J. L.; Vollenweider, L.; Xu, F.; Lee, B. P. Adhesive Performance of Biomimetic Adhesive-Coated Biologic Scaffolds. *Biomacromolecules* **2010**, *11* (11), 2976−2984.

(25) Michel, R.; Poirier, L.; van Poelvoorde, Q.; Legagneux, J.; Manassero, M.; Corté, L. Interfacial Fluid Transport Is a Key to Hydrogel Bioadhesion. *Proc. Natl. Acad. Sci. U. S. A.* **2019**, *116* (3), 738−743.

(26) Buwalda, S. J.; Nottelet, B.; Coudane, J. Robust & Thermosensitive Poly(Ethylene Glycol)-Poly(ε-Caprolactone) Star Block Copolymer Hydrogels. *Polym. Degrad. Stab.* **2017**, *137*, 173−183.

(27) Nouailhas, H.; Li, F.; El Ghzaoui, A.; Li, S.; Coudane, J. Influence of Racemization on Stereocomplex-Induced Gelation of Water-Soluble Polylactide-Poly(Ethylene Glycol) Block Copolymers. *Polym. Int.* **2010**, *59* (8), 1077−1083.

(28) Burns, A. B.; Register, R. A. Mechanical Properties of Star Block Polymer Thermoplastic Elastomers with Glassy and Crystalline End Blocks. *Macromolecules* **2016**, *49* (24), 9521−9530.

(29) Giuntoli, A.; Keten, S. Tuning Star Architecture to Control Mechanical Properties and Impact Resistance of Polymer Thin Films. *Cell Reports Phys. Sci.* **2021**, *2* (10), 100596.

(30) Liffland, S.; Hillmyer, M. A. Enhanced Mechanical Properties of Aliphatic Polyester Thermoplastic Elastomers through Star Block Architectures. *Macromolecules* **2021**, *54* (20), 9327−9340.

(31) Yang, J.; Cohen Stuart, M. A.; Kamperman, M. Jack of All Trades: Versatile Catechol Crosslinking Mechanisms. *Chem. Soc. Rev.* **2014**, *43*, 8271−8298.

(32) Sedõ, J.; Saiz-Poseu, J.; Busqué, F.; Ruiz-Molina, D. Catechol-Based Biomimetic Functional Materials. *Adv. Mater.* **2013**, *25*, 653−701.

(33) Hofman, A. H.; van Hees, I. A.; Yang, J.; Kamperman, M. Bioinspired Underwater Adhesives by Using the Supramolecular Toolbox. *Adv. Mater.* **2018**, *30*, 1704640.

(34) Grosjean, M.; Ouedraogo, S.; Déjean, S.; Garric, X.; Luchnikov, V.; Ponche, A.; Mathieu, N.; Anselme, K.; Nottelet, B. Bioresorbable Bilayered Elastomer/Hydrogel Constructs with Gradual Interfaces for the Fast Actuation of Self-Rolling Tubes. *ACS Appl. Mater. Interfaces* **2022**, *14* (38), 43719−43731.

(35) Assmann, A.; Vegh, A.; Ghasemi-Rad, M.; Bagherifard, S.; Cheng, G.; Sani, E. S.; Ruiz-Esparza, G. U.; Noshadi, I.; Lassaletta, A.

D.; Gangadharan, S.; Tamayol, A.; Khademhosseini, A.; Annabi, N. A Highly Adhesive and Naturally Derived Sealant. *Biomaterials* **2017**, *140*, 115−127.
(36) Chen, T.; Janjua, R.; McDermott, M. K.; Bernstein, S. L.; Steidl, S. M.; Payne, G. F. Gelatin-Based Biomimetic Tissue Adhesive. Potential for Retinal Reattachment. *J. Biomed. Mater. Res. - Part B Appl. Biomater.* **2006**, *77B* (2), 416−422.
(37) Saiz-Poseu, J.; Mancebo-Aracil, J.; Nador, F.; Busqué, F.; Ruiz-Molina, D. The Chemistry behind Catechol-Based Adhesion. *Angew. Chem., Int. Ed.* **2019**, *58*, 696−714.
(38) Lee, L.-H. New Perspectives in Polymer Adhesion Mechanisms-Importance of Diffusion and Molecular Bonding in Adhesion. *Proc. SPIE Adhesives Engineering* **1993**, *1999*, 6−21.
(39) Lee, B. P.; Dalsin, J. L.; Messersmith, P. B. Synthesis and Gelation of DOPA-Modified Poly(Ethylene Glycol) Hydrogels. *Biomacromolecules* **2002**, *3* (5), 1038−1047.
(40) Hoang Thi, T. T.; Lee, Y.; Le Thi, P.; Park, K. D. Engineered Horseradish Peroxidase-Catalyzed Hydrogels with High Tissue Adhesiveness for Biomedical Applications. *J. Ind. Eng. Chem.* **2019**, *78*, 34−52.
(41) Wang, D.; Xu, P.; Wang, S.; Li, W.; Liu, W. Rapidly Curable Hyaluronic Acid-Catechol Hydrogels Inspired by Scallops as Tissue Adhesives for Hemostasis and Wound Healing. *Eur. Polym. J.* **2020**, *134*, 109763.
(42) Lih, E.; Lee, J. S.; Park, K. M.; Park, K. D. Rapidly Curable Chitosan-PEG Hydrogels as Tissue Adhesives for Hemostasis and Wound Healing. *Acta Biomater.* **2012**, *8* (9), 3261−3269.
(43) Cencer, M.; Liu, Y.; Winter, A.; Murley, M.; Meng, H.; Lee, B. P. Effect of PH on the Rate of Curing and Bioadhesive Properties of Dopamine Functionalized Poly(Ethylene Glycol) Hydrogels. *Biomacromolecules* **2014**, *15* (8), 2861−2869.
(44) Buwalda, S. J.; Dijkstra, P. J.; Calucci, L.; Forte, C.; Feijen, J. Influence of Amide versus Ester Linkages on the Properties of Eight-Armed PEG-PLA Star Block Copolymer Hydrogels. *Biomacromolecules* **2010**, *11*, 224−232.
(45) Annabi, N.; Rana, D.; Shirzaei Sani, E.; Portillo-Lara, R.; Gifford, J. L.; Fares, M. M.; Mithieux, S. M.; Weiss, A. S. Engineering a Sprayable and Elastic Hydrogel Adhesive with Antimicrobial Properties for Wound Healing. *Biomaterials* **2017**, *139*, 229−243.
(46) Bian, S.; Zheng, Z.; Liu, Y.; Ruan, C.; Pan, H.; Zhao, X. A Shear-Thinning Adhesive Hydrogel Reinforced by Photo-Initiated Crosslinking as a Fit-to-Shape Tissue Sealant. *J. Mater. Chem. B* **2019**, *7* (42), 6488−6499.
(47) Marques, D. S.; Santos, J. M. C.; Ferreira, P.; Correia, T. R.; Correia, I. J.; Gil, M. H.; Baptista, C. M. S. G. Photocurable Bioadhesive Based on Lactic Acid. *Mater. Sci. Eng., C* **2016**, *58*, 601−609.
(48) Li, C.; Wang, T.; Hu, L.; Wei, Y.; Liu, J.; Mu, X.; Nie, J.; Yang, D. Photocrosslinkable Bioadhesive Based on Dextran and PEG Derivatives. *Mater. Sci. Eng., C* **2014**, *35* (1), 300−306.
(49) Ferreira, P.; Pereira, R.; Coelho, J. F. J.; Silva, A. F. M.; Gil, M. H. Modification of the Biopolymer Castor Oil with Free Isocyanate Groups to Be Applied as Bioadhesive. *Int. J. Biol. Macromol.* **2007**, *40* (2), 144−152.
(50) Ferreira, P.; Coelho, J. F. J.; Gil, M. H. Development of a New Photocrosslinkable Biodegradable Bioadhesive. *Int. J. Pharm.* **2008**, *352* (1−2), 172−181.
(51) Cholewinski, A.; Yang, F. K.; Zhao, B. Underwater Contact Behavior of Alginate and Catechol-Conjugated Alginate Hydrogel Beads. *Langmuir* **2017**, *33* (34), 8353−8361.
(52) da Silva, D.; Kaduri, M.; Poley, M.; Adir, O.; Krinsky, N.; Shainsky-Roitman, J.; Schroeder, A. Biocompatibility, Biodegradation and Excretion of Polylactic Acid (PLA) in Medical Implants and Theranostic Systems. *Chem. Eng. J.* **2018**, *340* (January), 9−14.
(53) Feng, P.; Jia, J.; Liu, M.; Peng, S.; Zhao, Z.; Shuai, C. Degradation Mechanisms and Acceleration Strategies of Poly (Lactic Acid) Scaffold for Bone Regeneration. *Mater. Des.* **2021**, *210*, 110066.
(54) Yamaoka, T.; Tabata, Y.; Ikada, Y. Distribution and Tissue Uptake of Poly(Ethylene Glycol) with Different Molecular Weights after Intravenous Administration to Mice. *J. Pharm. Sci.* **1994**, *83* (4), 601−606.
(55) U.S. Food & Drug Administration. https://www.accessdata.fda.gov/cdrh_docs/pdf/P990028b.pdf (accessed 2022−11−28).
(56) U.S. Food & Drug Administration. https://www.accessdata.fda.gov/cdrh_docs/pdf8/P080013b.pdf (accessed 2022−11−28).

SUPPORTING INFORMATION

Degradable bioadhesives based on star PEG-PLA hydrogels for soft tissue applications

Mathilde Grosjean[a], Edouard Girard[b,c,d], Audrey Bethry[a], Grégory Chagnon[b], Xavier Garric[a,e], Benjamin Nottelet[a]*

[a] *Polymers for Health and Biomaterials, IBMM, Univ Montpellier, CNRS, ENSCM, Montpellier, France*

[b] *Univ Grenoble Alpes, CNRS, CHU Grenoble Alpes, Grenoble INP, TIMC-IMAG, Grenoble, France*

[c] *Département de chirurgie digestive et de l'urgence, Centre Hospitalier Grenoble-Alpes, Grenoble, France*

[d] *Laboratoire d'anatomie des Alpes françaises (LADAF), UFR de médecine de Grenoble, Université Grenoble Alpes, Grenoble, France*

[e] *Department of Pharmacy, Nîmes University Hospital, 30900 Nîmes, France*

* benjamin.nottelet@umontpellier.fr

Content

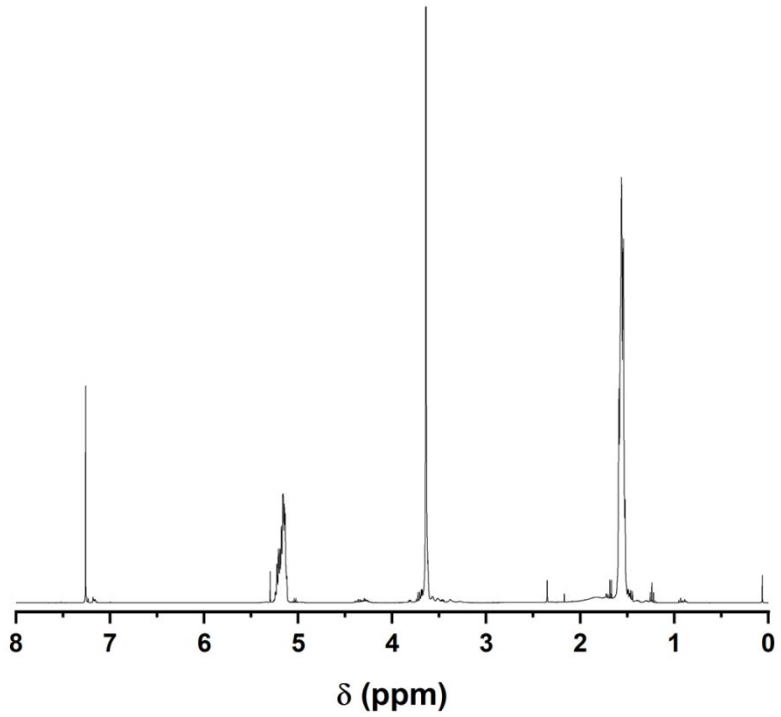

Figure S1. ^{1}H NMR spectrum of star-shaped PEG-PLA copolymer ($CDCl_3$).

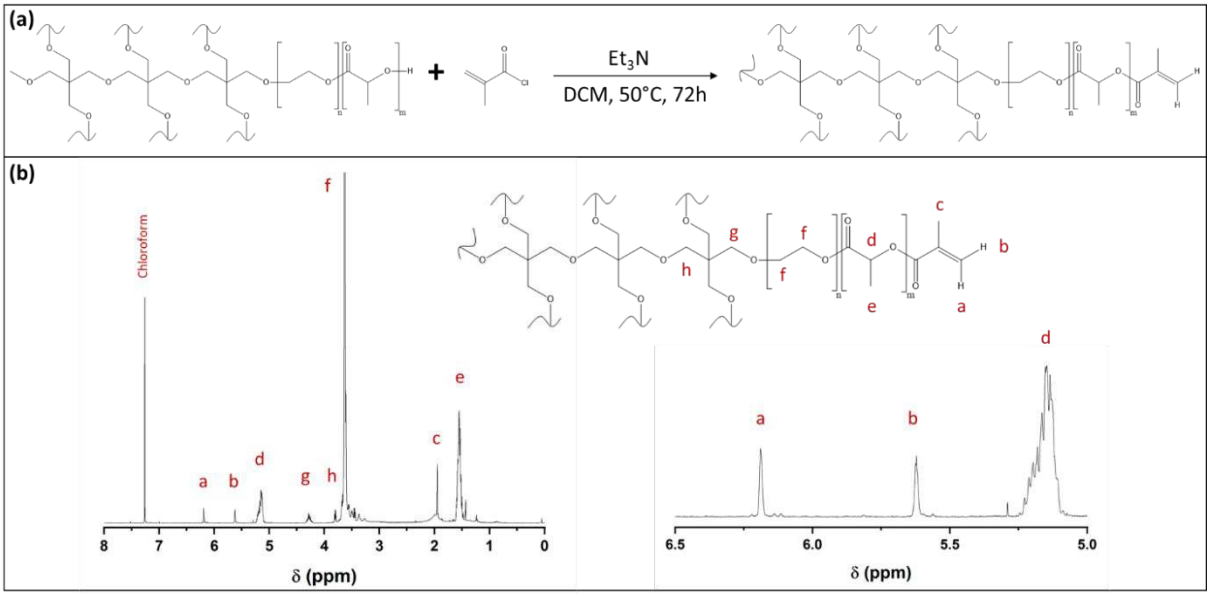

Figure S2. (a) Synthetic scheme of methacrylate functional copolymers (b) ^{1}H NMR spectrum of PEG_{s8}-PLA-MC.

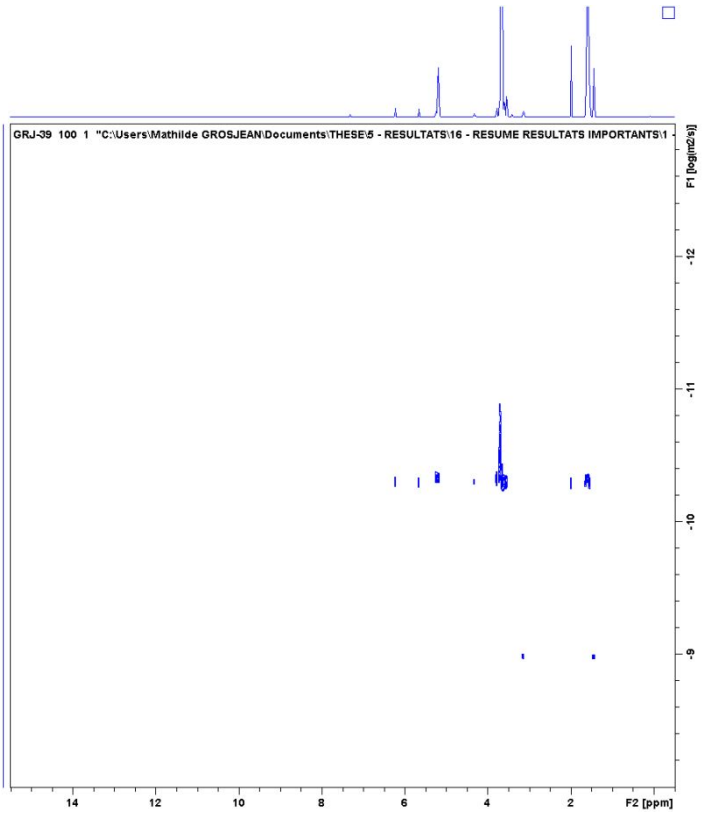

Figure S3. [1]H DOSY NMR spectrum of methacrylate functional PEG-PLA copolymer

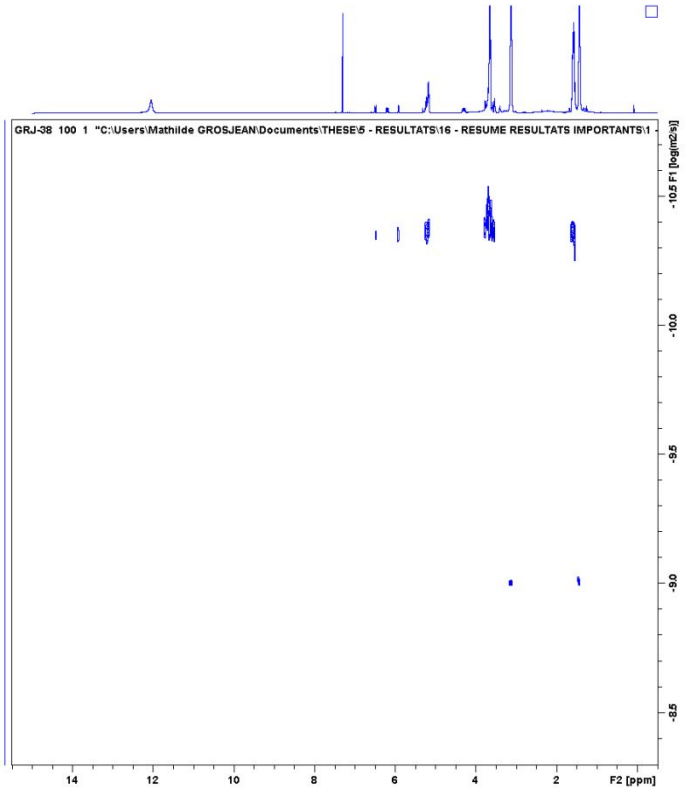

Figure S4. [1]H DOSY NMR spectrum of acrylate functional PEG-PLA copolymer

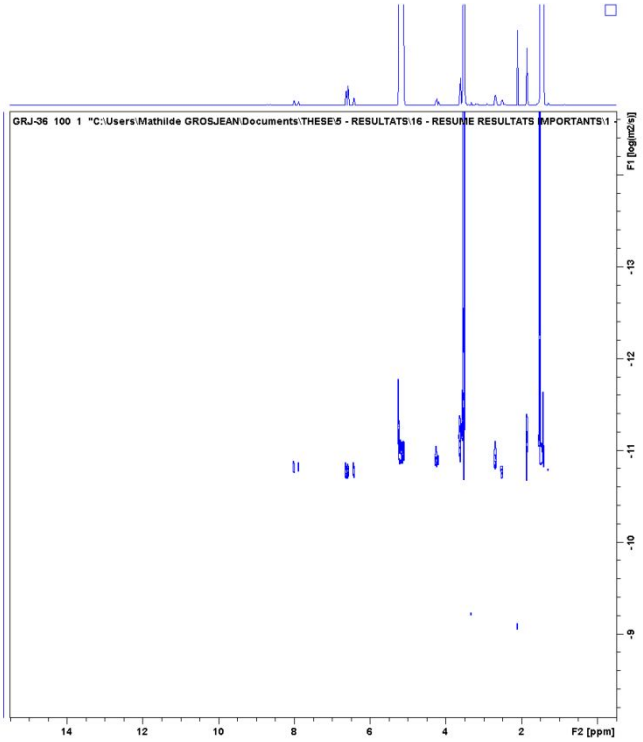

Figure S5. ^{1}H DOSY NMR spectrum of catechol functional PEG-PLA copolymer

Table S1. Values of viscosity (Pa.s) of solutions or hydrogels obtained by mixing PEG_{s8}-PLA-MC, PEG_{s8}-PLA-AC and PEG_{s8}-PLA-CT in water at different concentrations (5, 10, 15 and 20 wt%).

	5%	**10%**	**15%**	**20%**
PEG_{s8}-PLA-MC	$4.6\ 10^{-3}$	$2.2\ 10^{-2}$	$1.4\ 10^{-1}$	1.4
PEG_{s8}-PLA-AC	$9.2\ 10^{-3}$	$2.1\ 10^{-1}$	1.7	4.9
PEG_{s8}-PLA-CT	-	5.3	34.1	70.3

Appendix S1: Preliminary study of the adhesion properties of bioadhesives based on hybrid methacrylate-catechol functional star-shaped PEG-PLA hydrogels.

1. Synthesis of the copolymers

Hybrid methacrylate-catechol functional star-shaped PEG-PLA $PEG_{8arm}20k\text{-}(PLA_{13})_8$-MC/CT ($PEG_{s8}$-PLA-MC/CT) copolymers were synthesized by solubilizing determined amounts of dopamine hydrochloride (4 eq./methacrylate group) and citiolone (4 eq./methacrylate group) in DMF before adding Et_3N (8 eq./methacrylate group). The mixtures was then stirred overnight at room temperature before PEG_{s8}-PLA-MC was added (10% w/v) and to react at room temperature for 24 hours under stirring in the dark. The polymer was recovered by precipitation in cold Et_2O before being solubilized in DCM, washed with distilled water and concentrated. Afterwards, the mixture was precipitated in cold Et_2O a second time. The hybrid methacrylate/catechol PEG_{s8}-PLA-MC/CT was dried under reduced pressure to constant mass.

The functionalization was confirmed by ^1H NMR (DMSO-d_6).

The yield of functionalization was determined by comparing the integration of the methacrylate and catechol characteristic signal at 6.1 and 5.8 ppm and 6.6 and 6.4 ppm respectively and the integration of proton resonance at 3.6 ppm.

A functionalization degree of 30% regarding methacrylate functions and 70% regarding catechol groups was obtained.

2. Preparation of the gels

Non-oxidized hybrid gels were simply obtained by mixing PEG_{s8}-PLA-MC/CT with water at a concentration of 10 wt%.

Oxidized hybrid gels were prepared by mixing PEG_{s8}-PLA-MC/CT with $NaIO_4$ solution ($n_{catechol} = n_{NaIO4}$) at a concentration of 10 wt%.

3. Adhesive properties

The adhesive properties were evaluated on gelatin coating as described in section 2.5.1.

Values of adhesive strength of 65.4 and 87.8 kPa were obtained for non-oxidized and oxidized hybrid gels, respectively. These results are intermediate compared to those obtained for MC-Gel, CT-Gel and CT_{OX}-Gel.